RSC Advances

REVIEW

View Article Online
View Journal | View Issue

Cite this: *RSC Adv.*, 2023, **13**, 6713

Modified magnetic chitosan materials for heavy metal adsorption: a review

Ke Wang,[a] Fanbing Zhang,[a] Kexin Xu,[a] Yuju Che,[a] Mingying Qi[a] and Cui Song *[ab]

Magnetic chitosan materials have the characteristics of both chitosan and magnetic particle nuclei, showing the characteristics of easy separation and recovery, strong adsorption capacity and high mechanical strength, and have received extensive attention in adsorption, especially in the treatment of heavy metal ions. In order to further improve its performance, many studies have modified magnetic chitosan materials. This review discusses the strategies for the preparation of magnetic chitosan using coprecipitation, crosslinking, and other methods in detail. Besides, this review mainly summarizes the application of modified magnetic chitosan materials in the removal of heavy metal ions in wastewater in recent years. Finally, this review also discusses the adsorption mechanism, and puts forward the prospect of the future development of magnetic chitosan in wastewater treatment.

Received 9th November 2022
Accepted 7th February 2023

DOI: 10.1039/d2ra07112f

rsc.li/rsc-advances

1. Introduction

Heavy metals are beneficial to the development of industry and the quality of human life, such as their application in electroplating, steel manufacturing and textiles,[1] but excessive use has led to serious environmental and health problems. Toxic heavy metals migrate, transform, and accumulate in the biological chain, and these elements are harmful to human health.[2–4] For example, humans and animals can cause nerve damage if they consume too much copper.[5] High concentrations of lead ions can cause anorexia, irritability, constipation, abdominal pain, vomiting, reversible kidney damage, muscle weakness, anemia, encephalopathy, coma, and death.[6,7] Consuming too many chromium ions carries a risk of causing cancer.[5] Therefore, many researchers have developed effective and economical treatment technologies to reduce heavy metal ions in water sources. Common methods for reducing heavy metals in water matrices include catalytic oxidation, membrane separation, flocculation–sedimentation, adsorption, and biological methods.[5] Due to its simple operation, low cost, high removal efficiency, and environmental friendliness,[8] the adsorption method is considered to be a promising treatment method.

In recent decades, various natural and synthetic adsorbents have been examined for their ability to remove heavy metals from contaminated solutions.[9,10] Among various adsorbents, chitosan (CS) is widely used in the removal of heavy metals due to its excellent chemical properties, environmental friendliness and abundant adsorption sites.[11] Chitosan itself is a promising heavy metal adsorbent, but its adsorption capacity is limited due to its pH sensitivity and weak mechanical properties.[12] In addition, separating these adsorbents from water requires a complicated process and additional costs. Recently, magnetic adsorbents have attracted the interest of the scientific community because they can be easily separated from aqueous solutions.[13] Chitosan has polycation chelating properties in its surface amino groups and hydroxyl groups, which makes it a very advantageous material for functionalized magnetic nanoparticles.[14] In addition to the advantages of fast separation, the adsorption material modified by adding magnetic particles to chitosan also exhibits strong mechanical strength and excellent adsorption performance. Studies on magnetic chitosan adsorption have been summarized by some scholars (see Table 1). Briao *et al.*[15] focuses on the regeneration of adsorbents, Shaumbwa *et al.*[16] on the separation of magnetic materials, and Michailidou *et al.*[17] on the adsorption of highly toxic elements such as uranium and mercury. We focus on the adsorption of magnetic chitosan to common polluting metal ions (Cu/Pb/Cr). This paper not only compares the preparation methods and adsorption capacity of different magnetic chitosan materials but also discusses the environmental factors affecting the adsorption capacity and the corresponding adsorption mechanism. In particular, in the comparison of adsorption methods and capabilities, we review a large number of recent studies and compare the advantages and disadvantages of modification methods innovatively. Therefore, readers can understand the latest progress of magnetic chitosan more intuitively and provide necessary knowledge reserves for follow-up research.

2. Magnetic chitosan

Magnetic materials generally have high saturation magnetization, which can perform rapid and effective solid–liquid

[a]*Marine College, Shandong University, Weihai 264209, China. E-mail: songcui@sdu.edu.cn*
[b]*Shandong University-Weihai Research Institute of Industrial Technology, Weihai 264209, China*

Table 1 Comparison of the article with published article

	Aspect					
Article	Preparation method	Adsorb object	Adsorption evaluation	Adsorption mechanism	Novelty	Emphasis
The article	Coprecipitation method, crosslinking method, spray drying method, photochemical method and electrostatic drop method	Heavy metal ions (Cu, Pb, Cr)	BET surface area, adsorption capacity, pH, temp, cycles, kinetic and isotherm model	Physical adsorption, chemisorption and collaborative adsorption	Evaluate properties of magnetic chitosan prepared by different modification methods	Modification and application
Briao *et al.*[15]	Co-precipitation and crosslinking method	Toxic metal ions (Pb, Cd, Hg, As)	Kinetics, equilibrium and thermodynamics	—	Adsorbent regeneration	Magnetization method
Shaumbwa *et al.*[16]	Co-precipitation, crosslinking method and electrochemical crosslinking	Heavy metal ions, organic/inorganic dyes, fluorides and pesticides	Adsorption capacity, active sites and the surface area	—	Magnetic separation techniques	Application
Michailidou *et al.*[17]	Hydrothermal-crosslinking and hydrothermal-precipitation method	Uranium, mercury and rare earth elements	Kinetics and thermodynamics	Interaction between the functional group and the adsorbed substance	Adsorb uranium, mercury, and rare earth elements	Absorption efficiency

separation and avoid secondary pollution.[18] Magnetic chitosan mainly consists of two parts: chitosan and magnetic particles. Therefore, magnetic chitosan material has the dual characteristics of chitosan and magnetic materials. On the one hand, it has superparamagnetism and can be rapidly separated under an external magnetic field.[19] On the other hand, there are special functional groups that react with heavy metals, organics and other substances, which can be used as binding sites to improve the adsorption performance.[20] At present, magnetic chitosan materials have been studied and applied in many fields, such as environmental remediation,[21] biomedicine,[22] and petroleum exploitation.[23]

2.1 Chitosan

Chitosan is the only alkaline amylose in natural polysaccharides and is derived from chitin deacetylation in the cell walls of shrimp, crabs, insect shells, bacteria, and algae.[24,25] The uniqueness of the molecular structure of chitosan lies in the presence of a large number of hydroxyl and amino groups, which are effective adsorption sites for removing metal ions[26] (the structure and morphology are shown in Fig. 1a and b), and chitosan also has the characteristics of biodegradability and biocompatibility and does not easily cause secondary pollution, making it a better environmental functional material. However, chitosan has defects that limit its application in wastewater treatment. Therefore, people have tried to modify and improve performance through physical[27] or chemical modification methods[28] to improve its surface area and obtain more porosity and active sites.

2.2 Magnetic particles

Magnetic particles have a large specific surface area and therefore possess high surface energies and chemical activity, which are easily oxidized in air, resulting in the loss of magnetism and dispersion.[29] The addition of chitosan can maintain the stability of magnetic particles as a surface coating, reduce aggregation, prolong storage life, and improve the stability of the adsorbent.[30,31] Fig. 1c shows the typical shapes of several magnetic hybrid nanocomposites.[32]

Magnetic particles commonly include ferrite materials, such as MFe_2O_4 (M = Fe, Mn, Cu, Zn, Co, *etc.*), maghemite (γ-Fe_2O_3), magnetite (Fe_3O_4), *etc.* Among the various types of magnetic chitosan materials that have been reported, based on the excellent performance of Fe_3O_4, the most common magnetic particle used is Fe_3O_4, and the SEM micrographs are shown in Fig. 1d. In the study of magnetic factors affecting magnetic ions, it is found that the size of ionic magnetism is related to the band gap width of the semiconductor formed.[33] The results show that the magnetic properties in materials are caused by vacancy defects caused by surface electron transitions in the environment. This surface vacancy is the reason for the ferromagnetic coupling of materials. The material exhibits stable room-temperature magnetism only when the surface vacancy distance is approximately 8 A. Among the magnetic materials mentioned above, the Fe_3O_4 material has the most suitable surface vacancy distance, so it is the most ideal magnetic material to be doped. Compared with Fe_3O_4, a material obtained by substitution of crystal sites-MFe_2O_4 (M = Fe, Mn, Cu, Zn, Co, *etc.*) have a decrease in the hyperfine magnetic field, which can be significantly detected.[34] In magnetic studies, Fe_3O_4 shows ferromagnetism and Fe_2O_3 shows superparamagnetism. Compared with Fe_2O_3, the magnetization and coercivity fields of Fe_3O_4 samples are larger[35] due to their biocompatibility, high magnetic susceptibility, chemical stability, harmlessness, low cost and wide application, such as biomedicine,[36,37] water treatment,[38] catalysis.[39,40]

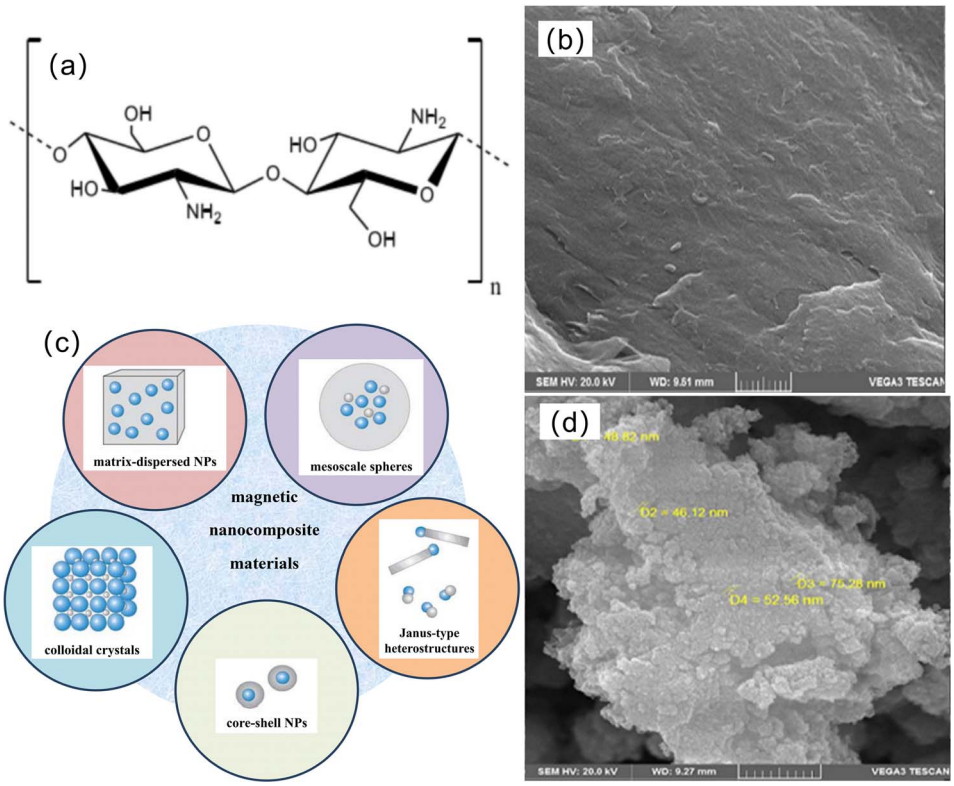

Fig. 1 (a) Chemical structure and (b) SEM micrographs of chitosan, (c) typical morphology of magnetic nanocomposites. The magnetic nanoparticle is represented by a blue ball. Gray represents non-magnetic entities and matrix materials, (d) SEM micrographs of Fe_3O_4.

3. Preparation of magnetic chitosan

There are many methods to synthesize magnetic chitosan, such as the coprecipitation method, crosslinking method, spray drying method,[41] photochemical method,[42] and electrostatic drop method. At present, two commonly used methods are the coprecipitation method and the crosslinking method.

3.1 Coprecipitation method

The coprecipitation method directly obtains uniform materials through chemical reactions in the solution, and the preparation process is simpler and more environmentally friendly than other methods. The coprecipitation method is divided into the *in situ* method and the two-step method.

3.1.1 *In situ* method. In the *in situ* method, chitosan microspheres were used as the core, infiltrated with chitosan microspheres in the form of Fe^{2+} and Fe^{3+} ions, and then synthesized *in situ* under alkaline conditions. Liu *et al.* used a simple one-pot coprecipitation method to prepare magnetic chitosan composites.[43] First, chitosan was dispersed in an acetic acid solution to obtain a chitosan solution, and then Fe^{3+} and Fe^{2+} ions were directly added. After uniform dispersion, sodium hydroxide or ammonia gas was added to control the pH to be alkaline and prevent the oxidation of Fe_3O_4 (Fig. 2a). Jumadi *et al.* added sodium dodecyl sulfate to partially reduce Fe^{3+} to Fe^{2+} to prepare magnetic chitosan[44] (Fig. 2b). Using the *in situ* method to prepare magnetic microspheres can not only keep the average particle size and particle size distribution coefficient of the polymer microspheres unchanged during the magnetization process but also ensure that the magnetic particles are uniformly distributed, showing consistent magnetic responsiveness.[45]

3.1.2 Two-step method. The two-step method is to first synthesize Fe_3O_4 magnetic nanoparticles and then use Fe_3O_4 as the core and wrap it with chitosan.

The important first step in the two-step method is to prepare magnetic particles. Fe_3O_4 nanoparticles can be easily synthesized by chemical coprecipitation,[46] in addition to the hydrothermal method,[47] pyrolyzis method,[48] sol–gel method,[49] and microemulsion method.[50] The chemical coprecipitation method to synthesize Fe_3O_4 magnetic nanoparticles mainly involves adding alkali into the Fe^{2+}/Fe^{3+} salt solution to provide an alkaline environment to generate Fe_3O_4. Its formation principle is formed through a nucleation and growth mechanism, as shown in Fig. 3a. The chemical coprecipitation method for synthesizing Fe_3O_4 has the advantages of being easy to implement and less harmful,[39] and the remaining synthetic methods are less commonly used on magnetic chitosan microspheres because of their complicated processes. The average particle size of Fe_3O_4 produced by the chemical coprecipitation method is less than 10 nm, but the magnetic nanoparticles themselves have a hydrophobic surface, so ion agglomeration is more serious, and Fe_3O_4 magnetic nanoparticles are particularly easy to oxidize, which usually leads to a decrease in magnetic properties and hinders the application

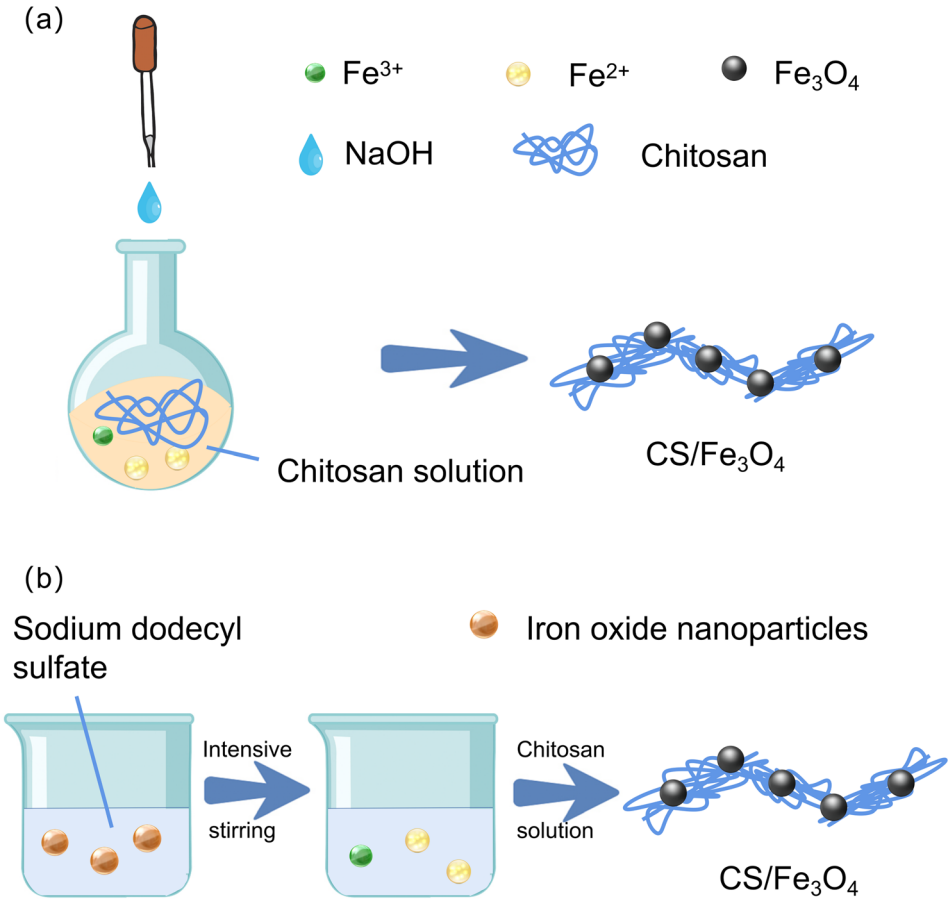

Fig. 2 (a and b) *In situ* synthesis steps of magnetic chitosan.

of magnetic chitosan microspheres. At present, Fe_3O_4 will be surface functionalized, and the strategies of surface functionalization can be roughly divided into surface modification of organic materials and inorganic materials. First, the functionalized magnetic nanoparticles on the surface of organic materials have a core–shell structure (Fig. 3b).[29] Second, modified with inorganic materials, nontoxic silica is a very ideal surface functional coating for magnetic nanoparticles.[51] Lu *et al.* synthesized Fe_3O_4@SiO_2 in an oxygen-free environment.[52] Jiang *et al.* synthesized magnetic Fe_3O_4@SiO_2-chitosan (MFSC)[53] (the synthesis process is shown in Fig. 3c). SiO_2 has strong acid resistance, and the core–shell structure formed with Fe_3O_4 enhances the stability and dispersion of magnetic chitosan microspheres (Fig. 3d). In recent years, the green synthesis of magnetic particles using plant extracts[54] such as tree bark extract,[55] coconut husk,[56] tekelan leaf,[57] neem leaf,[58] and Parkia speciosa Hassk pod extract has been widely developed. Plant extracts contain secondary metabolites such as phenolic compounds, tannins, and saponins. These compounds have hydrophobic properties and steric hindrance effects on metal surfaces, causing steric exclusion, which can control particle growth and prevent metal particle agglomeration during the synthesis process. The content of the –OH group in secondary metabolites can act as a reducing agent that maintains the balance of the Fe^{3+} and Fe^{2+} compositions in solution to produce magnetite (Fe_3O_4) with higher purity.[59] In addition, due to the particularity of raw materials, the magnetic materials prepared have some special functions. For example, Fe_3O_4 that prepared from water hyacinth (WH), also known as *Eichhornia crassipes* extract, can inhibit bacterial growth.[60] The existence of these special functions not only gives the material special properties, but also greatly improves the application range of the material.

The second step of the two-step method is to mix chitosan and Fe_3O_4 magnetic nanoparticles and use cross-linking, microemulsion and other methods to successfully encapsulate Fe_3O_4 magnetic nanoparticles in chitosan microspheres, giving the chitosan microspheres good magnetism. The cross-linking method uses a cross-linking agent to connect chitosan and Fe_3O_4 magnetic nanoparticles (Fig. 3e). Li *et al.* successfully embedded magnetite nanoparticles into chitosan beads through a two-step method, forming a porous structure (Fig. 3f).[61] The microemulsion rule is that the mixed solution of chitosan and Fe_3O_4 magnetic nanoparticles is slowly dropped into the microemulsion containing emulsifier and liquid paraffin, and the pH value is adjusted to alkaline for molding. Li *et al.* prepared magnetic chitosan microspheres by water-in-oil microemulsion polymerization.[62] The magnetic chitosan microspheres are typically spherical with smooth surfaces and no obvious defects, as shown in Fig. 3g.

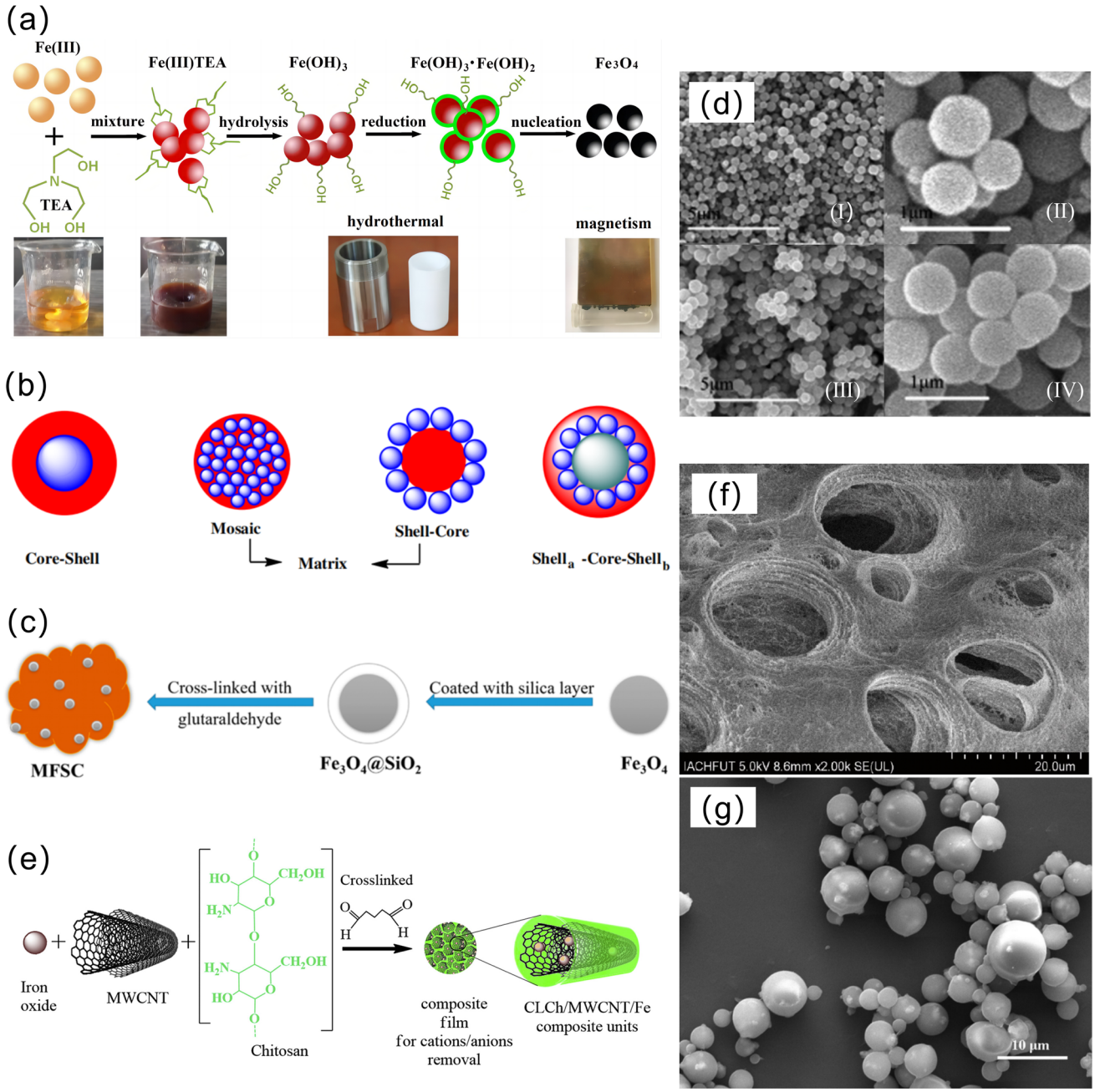

Fig. 3 (a) Schematic diagram of the formation mechanism of Fe_3O_4 magnetic nanoparticles, (b) the main structure of magnetic nanoparticles modified by organic materials, (c) Fe_3O_4@SiO_2-chitosan synthesis steps, (d) SEM images of the Fe_3O_4 (i and ii), Fe_3O_4@SiO_2 (iii and iv), (e) schematic diagram of the formation of magnetic chitosan nanocomposites by two-step method,[63] (f) SEM images of Fe_3O_4-CS beads, and (g) SEM images of magnetic chitosan microspheres.

3.2 Crosslinking method

The cross-linking method involves the formation of chemical bonds by the crosslinking agent to combine polymers (Fig. 4a). The crosslinking method is divided into two kinds according to the principle: chemical crosslinking and physical crosslinking (Fig. 4b). At present, the commonly used crosslinking agents for chemical crosslinking include glutaraldehyde, epoxy cross-linking agents and silane. The physical cross-linking agents used include polyphosphate, citric acid, κ-carrageenan and alginate. Table 2 lists the properties of common crosslinkers and composites formed. Different crosslinking agents will correspondingly affect the surface area and saturation magnetization of magnetic chitosan particles.

However, it is worth noting that most crosslinking agents are toxic and pose a certain risk to humans and organisms. In recent years, based on the development of green chemistry, the application of natural preparations in the synthesis of adsorption materials has been emphasized as an alternative method to

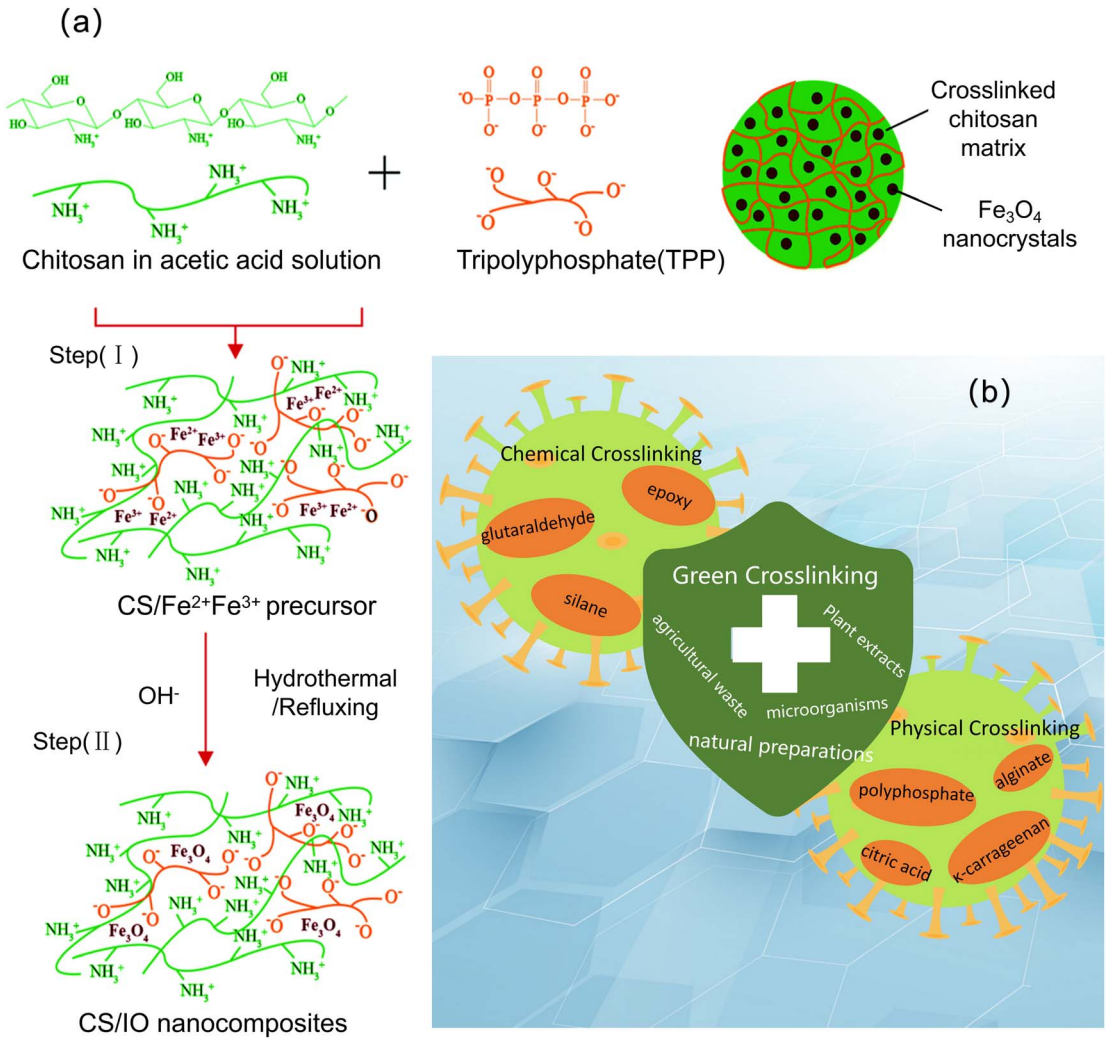

Fig. 4 Schematic diagram of magnetic chitosan synthesized by the (a) crosslinking method and (b) related crosslinking agents.

Table 2 Common crosslinking agents and properties of preparation materials[a]

Adsorbents	Crosslinker	Average size (nm)	BET surface area ($m^2\ g^{-1}$)	Saturation magnetization (emu g^{-1})	References
ZMChi/PVA	Glutaraldehyde	—	75.5	22	72
Bismuth ferrite/Biochar coupled magnetic material	Glutaraldehyde	—	6.78	0.95	73
CS/IO	Sodium tripolyphosphate (TPP)	3.9	—	14.5	63
mLCSCar0.2	κ-Carrageenan	16.7	—	29.1	74
CS-G/ZnO/Fe_3O_4 NPs	Glyoxal	7.3	10.706	23.37	75
Mag@PIA-*g*-CS	3-Trimethoxysilyl propylmethacrylate	—	—	51.9	76
CCMD	3-Aminopropyl trimethoxysilane	13–19	—	—	77

[a] Abbreviations: ZMChi/PVA:ZnO-coated MChi/PVA (ZMChi/PVA) microspheres; CS/IO: chitosan/iron oxide nanocomposites; mLCSCar0.2: ionically crosslinked magnetic chitosan/κ-carrageenan bioadsorbents; CS-G/ZnO/Fe_3O_4NPs: magnetically crosslinked chitosan-glyoxal/ZnO/Fe_3O_4 nanoparticles; Mag@PIA-*g*-CS: poly(itaconic acid-*g*-chitosan)-coated magnetic flocculant; CCMD: carboxymethyl chitosan-modified magnetic-cored dendrimers.

minimize the use of toxic chemical reagents.[64] Plant extracts, microorganisms and agricultural waste have a variety of active compounds and metabolites that can act as crosslinking agents in the synthesis processes, thus enabling the development of new composites with high efficiency, eco-friendliness and low cost. Queiroz *et al.* synthesized a composite material based on graphene oxide and magnetic chitosan using a green route with procyanidins as a crosslinking agent.[65] Liu *et al.* synthesized

a magnetic chitosan three-dimensional biosorbent for the removal of methylene blue using agricultural waste corn stalk core as a scaffold and green crosslinking.[66] Some researchers have also used special crosslinking agents and methods to achieve non-toxic crosslinking. Wang *et al.* synthesized a nanocomposite magnetic attapulgite using ethylene diaminetetraacetic acid (EDTA) as a crosslinking agent. EDTA is safe and nontoxic, in line with the concept of a green synthetic adsorbent. Anchali *et al.* synthesized magnetic chitosan-magnetite gel microparticles using ethylene glycol diglycidyl ether (EDGE) as a green and safe crosslinking agent.[67] Rahmi *et al.* used sulfuric acid as a cross-linking agent to synthesize magnetic chitosan nanocomposite beads.[68] The crosslinking process using H_2SO_4 produces chitosan chains that form strong antiparallel structures and hydrogen bonds,[69] which increases the adsorption capacity and stability of chitosan and acid resistance and reduces the crystallinity properties.[70] Deniz *et al.* proposed a new method for preparing magnetic Fe_3O_4-chitosan micronanoparticles (Fe_3O_4-CNs) using a traditional suspension cross-linking method.[71] Different from ordinary synthesis methods, they use ultrasonic treatment to control the synthesis of particles during the particle synthesis process and obtain the desired characteristics.

3.3 Other methods

In addition to the above two methods, some other methods can also be used to prepare magnetic chitosan materials, such as the spray drying method, photochemical method, and electrostatic drop method. The preparation process of the spray-drying and photochemical methods is shown in Fig. 5a. The electrostatic drop method is a combination of electrostatic drop (ESD) technology and a chemical cross-linking process for synthesis. Xu *et al.* used the electrostatic drop method to fabricate Fe_3O_4 nanoparticle-embedded porous chitosan microspheres (Fe_3O_4/PCSM),[78] as shown in Fig. 5b. Together with the pumping action, the microscopic ferro-gels, which contain ferrous cations, ferric cations and chitosan, can be accelerated downward along the electric field strength gradient and transferred to an alkaline solution for curing. The as-prepared Fe_3O_4/PCSM exhibits a good spherical shape and large channels, uniform dispersion, and easy separation.

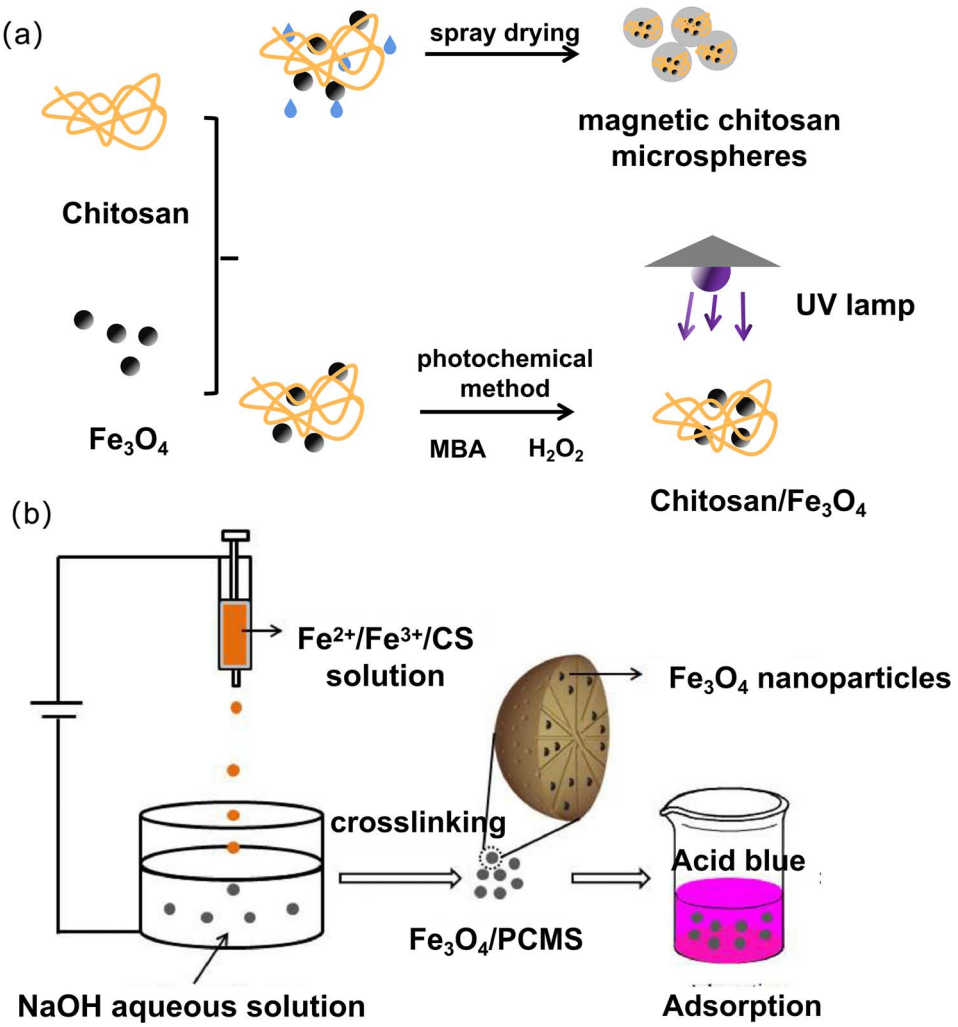

Fig. 5 Schematic diagram of magnetic chitosan synthesized by (a) spray drying and photochemical method, (b) electrostatic drop method.

4. Application of modified magnetic chitosan materials in heavy metal adsorption

Heavy metals occupy an important position in daily industrial production, but their excessive use and consumption seriously damage the environment and pose a serious threat to human health. Compared with chitosan, magnetic chitosan has more advantages in separation, recovery, mechanical strength and good adsorption. It has gradually become a promising adsorbent for heavy metals. This section summarizes the research and application of magnetic chitosan in the removal of heavy metal ions in recent years.

The adsorption capability of a treatment material can be evaluated by adsorption capacity. Isotherm studies can provide information regarding the maximum adsorption capacity, which helps to compare performance between different adsorbents. Most metal ion adsorption can be fit with Langmuir or Freundlich isotherm models. The Langmuir model assumes monolayer adsorption, while the Freundlich model assumes a heterogeneous surface.[79]

4.1 Adsorption of Cu

Copper (Cu) and its compounds have been used as algaecides in aquaculture, as absorbents in carbon dioxide capture technology, *etc.*[80–82]. Although various cellular processes utilize copper as an enzyme cofactor,[83] excessive copper ions have been found to inhibit plant growth and root development. Moreover, high copper intake in humans and animals has been linked to various forms of physiological and neurological damage.[5,84,85] The World Health Organization (WHO) sets the maximum allowable limit for Cu(II) in drinking water at 2 mg L^{-1};[86] however, in actual industrial production, a large amount of Cu will be emitted, causing inevitable damage to the environment. Therefore, the treatment of copper is necessary.

Table 3 The adsorption capacity of magnetic chitosan and its derivatives for Cu(II)[a]

Adsorbent	Ion concentration (mg L^{-1})	BET surface area (m^2 g^{-1})	Adsorption capacity of Cu(II) (mg g^{-1})	pH; temp (° C)	Kinetic model	Isotherm model	Cycles	Advantages	Reference
MCC	2	—	216.8	6; 25	Pseudosecond-order	Langmuir	6	Easy to separate, recycle and reuse	87
CMLB	40	104.91	54.68	5.8; —	Pseudosecond-order	Freundlich	3	Good removal efficiency and environmentally friendly	88
PCCM	100	—	81.3	5.5; —	Pseudosecond-order	Langmuir	7	Easily separate and use multiple cycles	89
CMFO	200	—	14.86	4.5; 25	Pseudosecond-order	Langmuir	—	Prepared without the use of toxic crosslinkers	90
MCSB	60	—	124.53	—; —	Pseudosecond-order	Langmuir	—	Satisfactory mechanical properties, good magnetic properties and easy to separate	91
CCMF	100	68.0	115.65	6; 25	Pseudosecond-order	Langmuir	—	High adsorption capacity	92
MCTS-Ag/Bi_2WO_6	50	—	68.68	6; —	Pseudosecond-order	Freundlich	5	Photo-assisted adsorption removal	93
MCMAs	100	—	119.21	—; —	Pseudosecond-order	Langmuir	4	Relatively high adsorption capacity, microorganisms assist in removal	94
ECSBNC	100	—	90.90	—; —	Pseudosecond-order	Langmuir	—	Nitrogen-containing functional groups improve adsorption capacity	95
MCGON	100	132.9	217.4	8; 25	Pseudosecond-order	Langmuir	5	Excellent adsorption capacity, high specific surface area, superparamagnetic	96
Fe_3O_4-CS/EDTA	200	2.622	225.0	—; —	Pseudosecond-order	Langmuir	8	Simultaneous capture of two types of pollutants	97

[a] Abbreviations: MCC: chitosan matrix embedding magnetite/maghemite; CMLB: chitosan-combined magnetic biochar; PCCM: porous and shape-adjustable magnetic aerogel based on PCs, chitosan and Fe_3O_4;CMFO: $MnFe_2O_4$/chitosan nanoadsorbents; MCSB: magnetic chitosan/sodium alginate gel bead; CCMF: chitosan-cellulose enwrapped magnetic carbon foam; MCTS-Ag/Bi_2WO_6: magnetic chitosan@bismuth tungstate coated by silver; MCMAs: the magnetic chitosan microspheres immobilized on *Aspergillus sydowii*; ECSBNC: epichlorohydrin crosslinked chitosan Schiff base-Fe_3O_4 nanocomposite; MCGON: magnetic chitosan/graphene oxide nanocomposite; Fe_3O_4-CS/EDTA: magnetic chitosan composite adsorbent functionalized with EDTA.

We will introduce the relevant studies with great characteristics in detail as follows. Many materials with good adsorption properties are summarized in Table 3; for example, the adsorption capacities of Fe_3O_4-CS/EDTA and MCGON were larger, MCC and PCCM were easier to recycle, and the technology for removing copper ions in wastewater has been extensively studied. And for the adsorption process of Cu ions, most materials conform to the Langmuir model and pseudosecond-order model.

On the basis of magnetic chitosan, many studies have enhanced the adsorption capacity of magnetic chitosan by compounding other substances to improve the structure of chitosan and combining and assisting synergy. Chen *et al.* developed a multifunctional EDTA-functionalized magnetic chitosan composite adsorbent (Fe_3O_4-CS/EDTA) for the simultaneous removal of methyl blue (MB) and heavy metals (Pb(II) and Cu(II)) in complex wastewater.[97] The adsorbent has synergistic removal performance for cationic metal ions and anionic dyes. The EDTA chelating group is mainly responsible for the binding of heavy metals, while the protonated amino group of CS adsorbs anionic dyes through electrostatic interactions. With increasing pH, the uptake of Cu(II) and Pb(II) increases

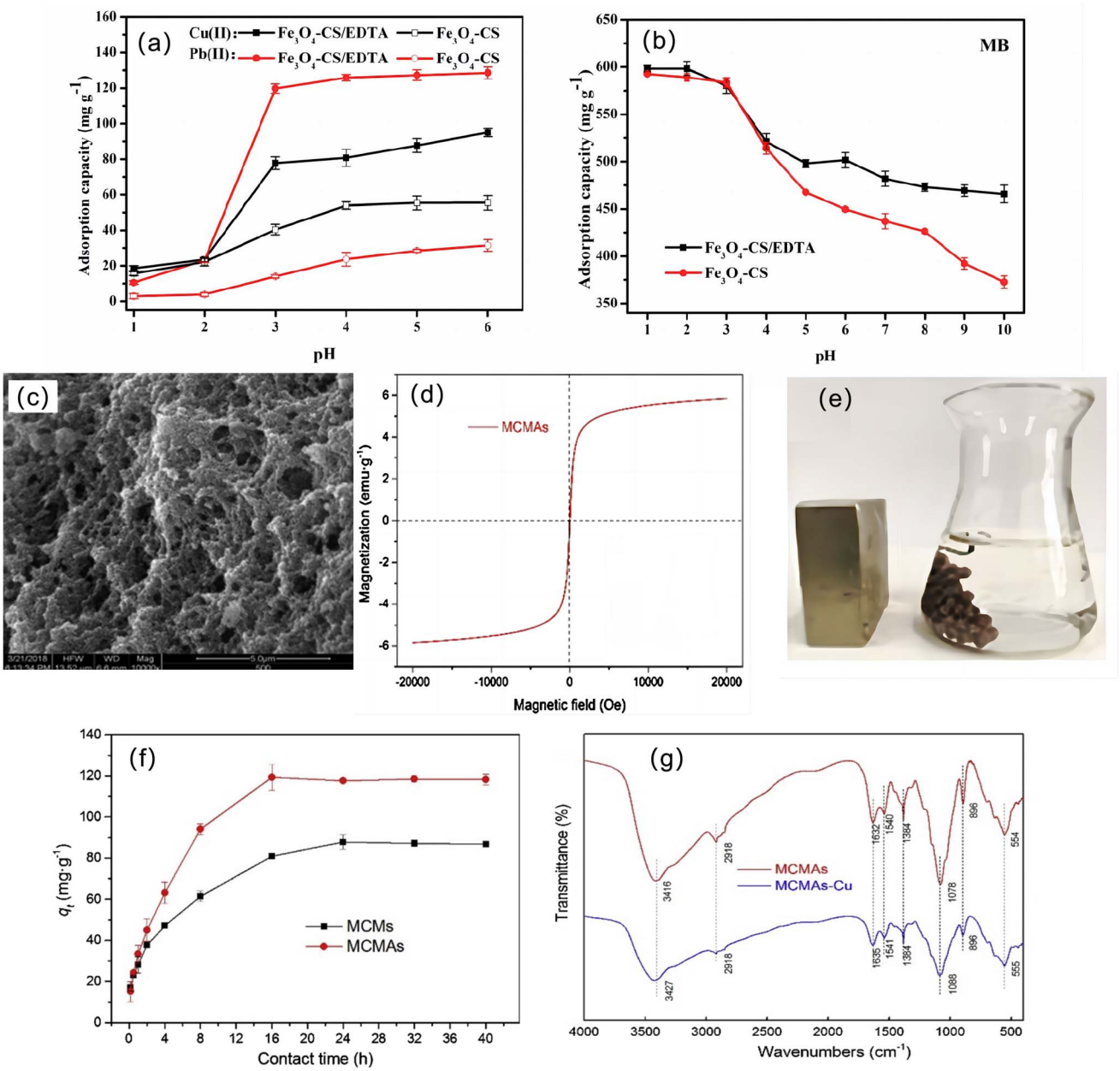

Fig. 6 Effect of solution pH on sorption of Fe_3O_4-CS and Fe_3O_4-CS/EDTA toward heavy metals (a) and MB (b), (c) internal SEM images of MCMAs, (d) magnetization curve of MCMAs, (e) magnetic separation of MCMAs, (f) effect of contact time on Cu(II) removal, and (g) FT-IR spectra of MCMAs before and after Cu(II) adsorption.

gradually. MB is the opposite, which is related to the different adsorption mechanisms, but it can be seen that the modification of EDTA makes Fe_3O_4-CS have a higher adsorption performance for heavy metals and MB over a wide pH range (Fig. 6a and b). The removal of heavy metal ions from wastewater using magnetic chitosan as a microbial immobilization carrier has been reported.[98,99] Magnetic chitosan microspheres immobilized on Aspergillus (MCMAs) were prepared by Zhang *et al.*[94] MCMAs show obvious interconnected porous structures (Fig. 6c), indicating that they can provide a large number of adsorption sites for heavy metals, showing excellent immobilization properties.[100] The magnetic properties of MCMA are shown in Fig. 6d and e. This indicates that MCMAs have good superparamagnetic properties and show good recycling potential.[101] The addition of *A. sydowii* made the adsorption performance of MCMAs significantly higher than that of unadded MCMs (Fig. 6f). First, the mycelia of immobilized *A. sydowii* stretched to fill the voids of MCMA after incubation, resulting in a denser structure and increasing the specific surface area. Second, the cell wall of *A. sydowii* is composed of various functional groups, such as hydroxyl-, amino-, carboxyl-, and phosphate-[102,103] and it is also confirmed that these groups are indeed involved in Cu(II) chelation (Fig. 6g). Third, microbial surfaces are often negatively charged, thereby contributing adsorption sites for binding metal ions.[104] Hosseinzadeh and Ramin *et al.* studied the performance of magnetic CS/graphene oxide nanocomposites (MCGONs) for copper ion removal in detail.[96] The introduction of graphene oxide (GO) significantly improves the adsorption performance of the material for Cu^{2+} ions, which is due to the presence of hydrophilic oxygenated groups such as –COOH, –C═O, –OH, and –C—O—C– on the surface of GO nanosheets. Fig. 7a shows the effect of GO nanosheets on Cu removal. With the prolongation of stirring time, the adsorption capacity of the adsorbent increases, and the whole adsorption conforms to the Langmuir isotherm (Fig. 7b).

In addition, some studies have also used other magnetic particles to improve the adsorption performance of magnetic

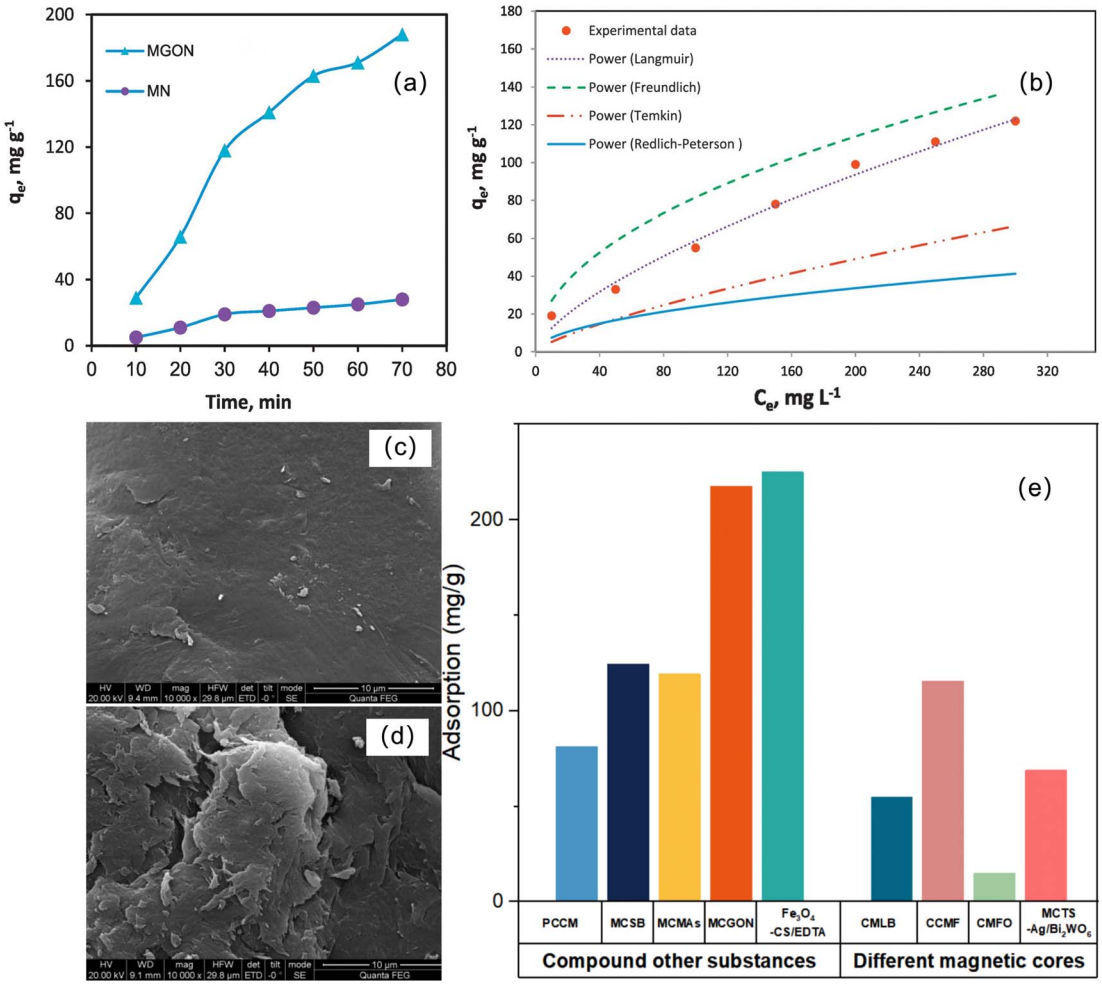

Fig. 7 (a) Effect of graphene oxide on the Cu^{2+} adsorption capacity of MCGON adsorbent, (b) comparison between the experimental and modeled isotherm plots for the adsorption of Cu^{2+} onto the MCGON adsorbent, SEM images showing the surface morphology of the (c) chitosan and (d) chitosan-cellulose hydrogel beads, (e) adsorption capacity diagram of magnetic chitosan materials modified by different methods of Cu(II).

chitosan by replacing Fe_3O_4 magnetic particles. Taguba *et al.* synthesized magnetic chitosan—manganese ferrite (CMFO) by simple low-temperature combustion technology without a toxic crosslinking agent.[90] The surface of CMFO is rough, and agglomerated particles appear. The maximum adsorption capacity of Cu on CMFO is 14.86 mg g^{-1}, and the adsorption process is spontaneous and endothermic, which is consistent with the Langmuir model. Zhang *et al.* prepared a novel adsorbent of chitosan-cellulose enwrapped magnetic carbon foam (CCMF).[92] Cellulose increases the specific surface area and porosity of the material (Fig. 7c and d), and the magnetic carbon foam makes the adsorbent lighter, making it float in water during the adsorption process, reducing the energy consumption of mechanical stirring which improves the adsorption performance and adsorption rate of metal ions.

In view of the above two kinds of modification methods, according to the comparative analysis of Fig. 7e, we found that for the modification of copper ion adsorption materials, the composite effective material to improve the material structure is better than the replacement of the magnetic core to obtain better adsorption performance, especially by introducing the material that can greatly increase the number of adsorption groups, such as Fe_3O_4-CS/EDTA and MCGON.

4.2 Adsorption of Pb

Lead (Pb) is the main component of batteries, ammunition and paint and is widely used in industrial production,[105–107] but Pb is extremely toxic to humans. The International Agency for Research on Cancer has categorized lead-containing inorganic compounds under "Group 2A: probably carcinogenic to humans".[108] The United States Environmental Protection Agency has set interim drinking water health advisory levels of 0.015 mg L^{-1} for Pb^{2+} ions.[109] However, lead is poisonous to living organisms when it is taken even at trace levels[110,111] and

Table 4 The adsorption capacity of magnetic chitosan and its derivatives for Pb(II)[a]

Adsorbent	Ion concentration (mg L^{-1})	Adsorption capacity of Pb(II) (mg g^{-1})	pH; temp. (°C)	Kinetic model	Isotherm model	Cycles	Advantages	Reference
MCS-Sch	10	121.95	5; —	—	Freundlich	7	The simplicity and minimum usage of the toxic compounds	113
TEPA/CS/$CoFe_2O_4$	200	228.3	5; 30	Pseudosecond-order	Langmuir	—	High magnetization, efficient adsorption performance	114
MCS-PAA	100	204.89	6; —	Pseudosecond-order	Langmuir	5	Excellent acid resistance	115
$(Fe_3O_4/CS\text{-}Se)_2$	100	100.3	6; —	—	—	4	Easy to separate, short extraction times and less adsorbent	116
HA-MG-CH	150	144.41	5; 25	Pseudosecond-order	Sips	5	Effective reduction of metal ions below allowable levels	117
Pb(II)-IMB	200	69.48	5; —	Pseudosecond-order	Langmuir	5	Efficient adsorption, good selectivity, and convenient magnetic separation	118
CH-MNP-CA	—	192.308	6.1; —	Pseudosecond-order	Langmuir	5	No secondary waste production, high saturation magnetization	119
MGC	25	60.60	7; 60	Pseudosecond-order	Langmuir	—	Applied to two fields with good adsorption performance	120
P-MCS	40	151.06	6; 45	Pseudosecond-order	Langmuir	5	Excellent magnetic separation and regeneration performance, cost savings	121
FFO@Sil@Chi-DTPA	—	322.58	6; —	Pseudosecond-order	Langmuir	—	Excellent selective adsorption of multiple pollutants	122
CHT/ALG/Fe_3O_4@SiO_2	180	234.77	4.2; 20	Elovich	Langmuir		Simple and innovative preparation, stable in acid water system	123
MCF3DG	16	—	8.5; —	—	—	5	Lightweight with good strength and weight resistance, good magnetic response, non-toxic properties	124

[a] Abbreviations: MCS-Sch: magnetic chitosan-(D-glucosamine methyl)benzaldehyde; MCS-PAA: polyacrylic acid grafted magnetic chitosan nanocomposite; $(Fe_3O_4/CS\text{-}Se)_2$: diphenyl diselenide onto chitosan carrying magnetite (Fe_3O_4) nanoparticles; HA-MG-CH: grafted hydrazinyl amine magnetite-chitosan; Pb(II)-IMB: lead-ion-imprinted magnetic biosorbent; CH-MNP-CA: chitosan-conjugated magnetite nanobiocomposite; MGC: magnetic nanobiocomposite based on activated chitosan-magnetic guanidinylated chitosan nanobiocomposite; P-MCS: phosphorylated magnetic chitosan composite; FFO@Sil@Chi-DTPA: DTPA-modified chitosan-coated magnetic silica nanoparticle; CHT/ALG/Fe_3O_4@SiO_2: magnetic chitosan/alginate/Fe_3O_4@SiO_2 hydrogel composites; MCF3DG: novel magnetic three-dimensional graphene/chitosan/nickel ferrite nanocomposite.

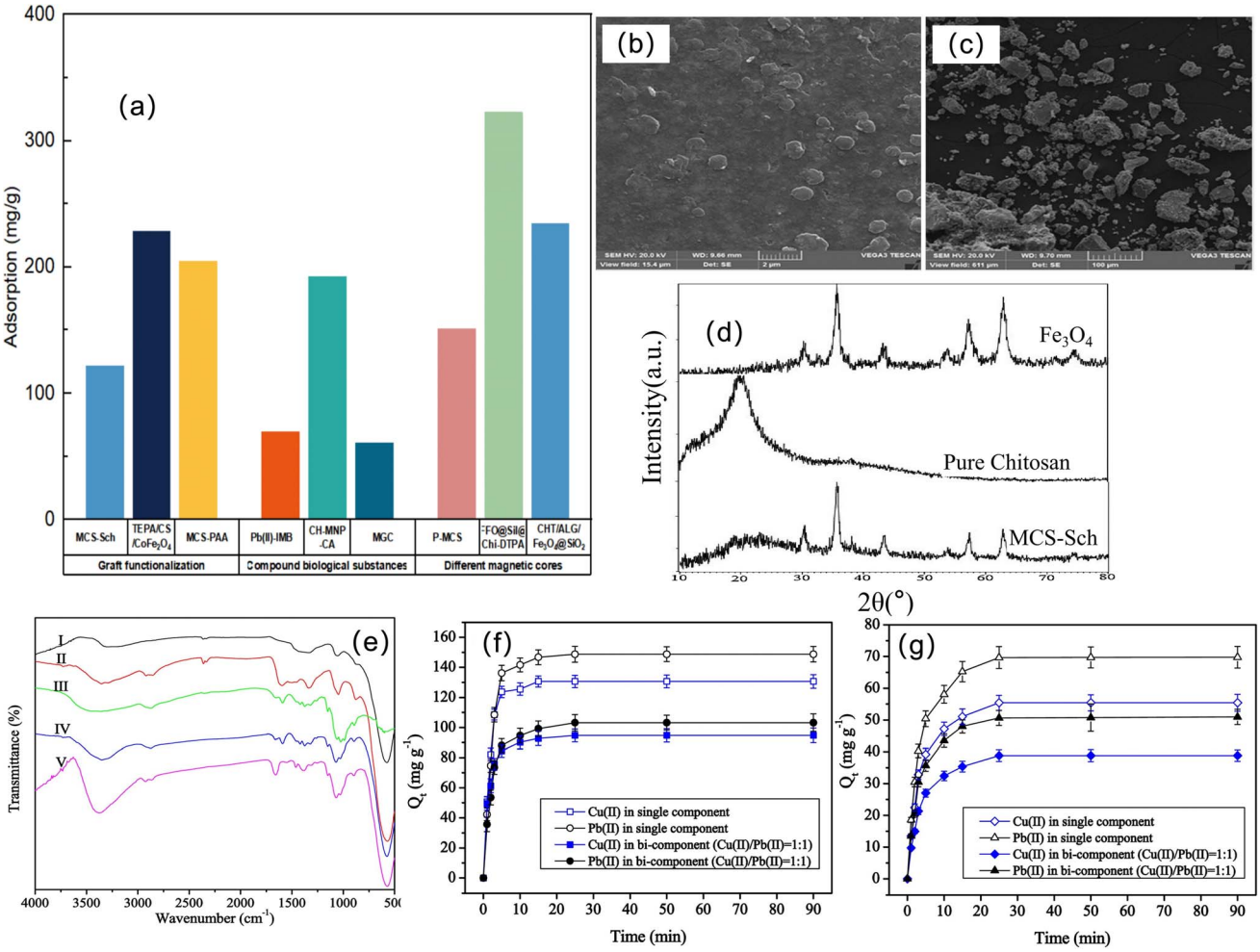

Fig. 8 (a) Adsorption capacity diagram of magnetic chitosan materials modified by different methods of Pb(II), (b and c) SEM micrographs of MCS-Sch, (d) XRD patterns of Fe_3O_4, chitosan and MCS-Sch, (e) FTIR spectra of (i) $CoFe_2O_4$, (ii) amine-$CoFe_2O_4$, (iii) chitosan, (iv) chitosan/$CoFe_2O_4$ and (v) TEPA modified chitosan/$CoFe_2O_4$, (f) adsorption kinetics of Cu(II) and Pb(II) on chitosan/$CoFe_2O_4$, and (g) adsorption kinetics of Cu(II) and Pb(II) on TEPA modified chitosan/$CoFe_2O_4$.

lead ions in the environment are difficult to degrade, so removing Pb(II) from the environment is an attractive issue.[112]

At present, the magnetic chitosan adsorbents for lead ions can be roughly divided into three types. One is to introduce groups through grafting and functionalization and exert a synergistic effect to enhance the adsorption of Pb ions. Another type is the preparation of biosorbent materials by combining biological substances. The last type is magnetic chitosan using other magnetic substances. We summarize these materials in Table 4. It can be seen that these adsorbents have generally better performance, among which FFO@Sil@Chi-DTPA has the largest adsorption capacity, and MCS-Sch can achieve the maximum number of cycles. For the adsorption process of Pb ions, most materials conform to the Langmuir model and pseudosecond-order model. From Fig. 8a, it can also be seen that for the adsorption of lead ions, materials modified with other magnetic substances have better adsorption effects than the other two methods, and the improvement in performance of different magnetic cores is inconsistent. The reason for the higher adsorption capacity of FFO@Sil@Chi-DTPA is related not only to the magnetic core, but also to the functional modification of DTPA. At the same time, grafting functionalization is generally superior to the means of composite biomass, which has a great relationship with the number of effective adsorption sites. However, we should also affirm the versatility of biosorbent materials, such as MGC, for cancer hyperthermia.

The first type is graft functionalization. Graft functionalization can greatly improve the adsorption properties of magnetic chitosan,[125] and many different reactive groups have been used to decorate polymers, including EDTA and analogs,[126] amino acids,[127] amidoxime,[128] and aminophosphonate.[129] Shahraki *et al.* synthesized a magnetic chitosan nanocomposite material based on Schiff base functionalization: MCS-Sch.[113] The surface of MCS-Sch is rough, magnetic Fe_3O_4 nanoparticles are embedded or mounted inside CS-Sch (Fig. 8b and c), and the crystal structure of Fe_3O_4 is not destroyed after MCS-Sch formation (Fig. 8d). As the pH value increases, the removal

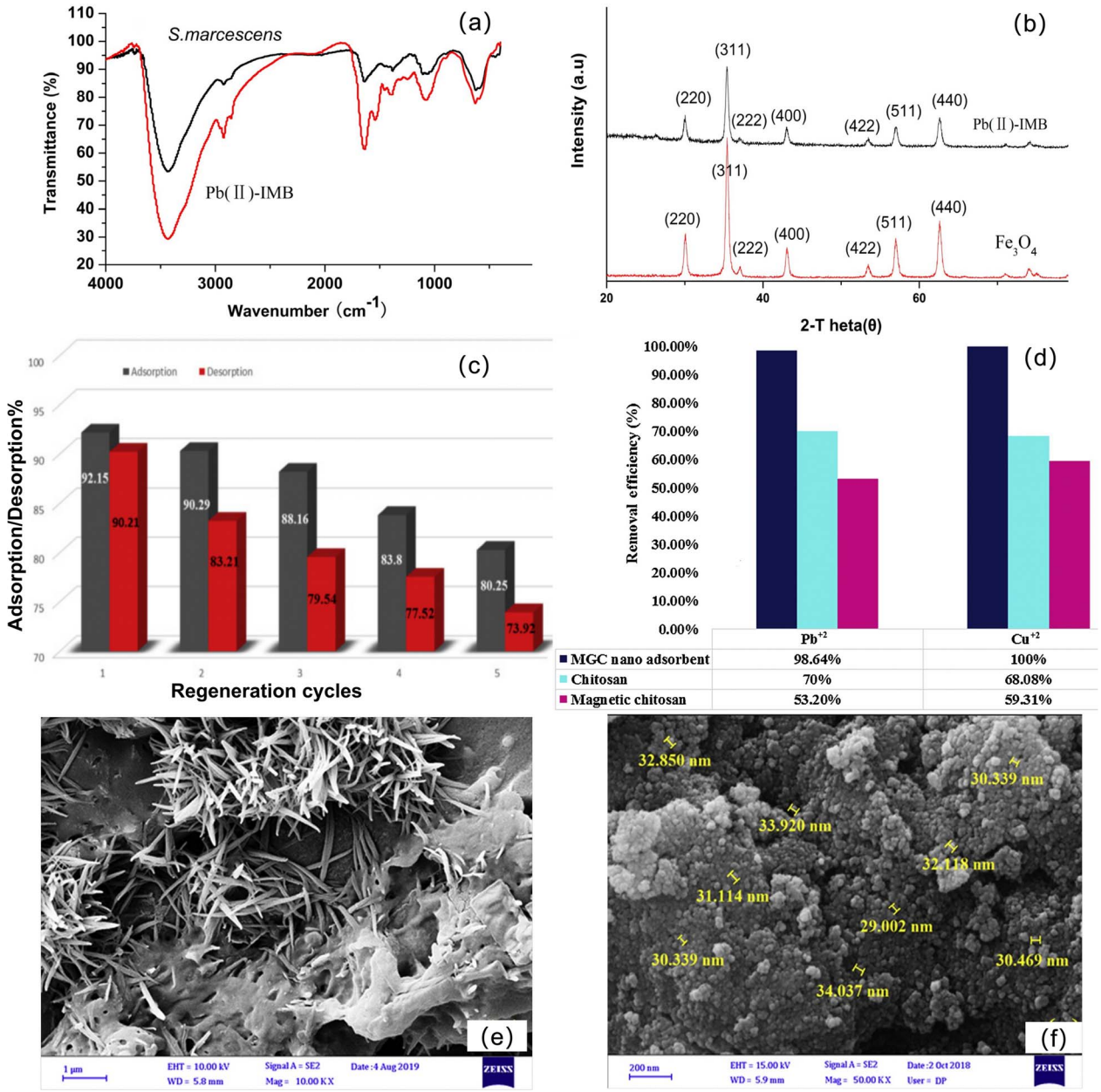

Fig. 9 (a) FT-IR of Pb(II)-IMB and *S. marcescens*, (b) XRD spectra of Pb(II)-IMB and Fe_3O_4, (c) desorption and adsorption of CH-MNP-CA nano-adsorbents over five runs, (d) comparison chart of removal efficiency percentage of unmodified chitosan, magnetic chitosan and MGC nano-adsorbent in adsorption of Cu^{2+} and Pb^{2+} ions, (e) FE-SEM images of guanidinylated chitosan, (f) FE-SEM images of MGC nanobiocomposite.

percentage of Pb(II) increases. The advantage of this material is that the presence of azomethine and aromatic rings can enhance the ability of MCS-Sch to interact with metal ions. Fan *et al.* used tetraethylenepentamine (TEPA) to further modify magnetic CS/$CoFe_2O_4$ for the adsorption of Pb(II) (or Cu(II)) in one- and two-component solutions.[114] The spectrum of chitosan/$CoFe_2O_4$(IV) was compared with that of TEPA-modified chitosan/$CoFe_2O_4$(V), as shown in Fig. 8e. It can be seen that a strong peak appears at 1655 cm^{-1}, indicating that TEPA modification will generate more amino groups that can bind metal ions, resulting in better adsorption performance. Fig. 8f and g shows the effect of contact time on the adsorption capacity of Cu(II) (or Pb(II)) in single and bicomponent (Cu(II)/Pb(II) = 1 : 1) solutions on chitosan/$CoFe_2O_4$ and TEPA-modified chitosan/$CoFe_2O_4$. It was obvious that the uptakes of Cu(II) and Pb(II) on chitosan/$CoFe_2O_4$ were evidently improved after TEPA modification.

The second is combining biological substances to make magnetic chitosan bioadsorbent materials. He *et al.* synthesized a novel biological material with high adsorption capacity and good selectivity for Pb^{2+}: lead-ion-imprinted magnetic biosorbent (Pb(II)-IMB).[118] FT-IR shows that Pb(II)-IMB is rich in adsorbable groups or sites, which are favorable for the adsorption of metal ions (Fig. 9a). In addition, XRD showed that the

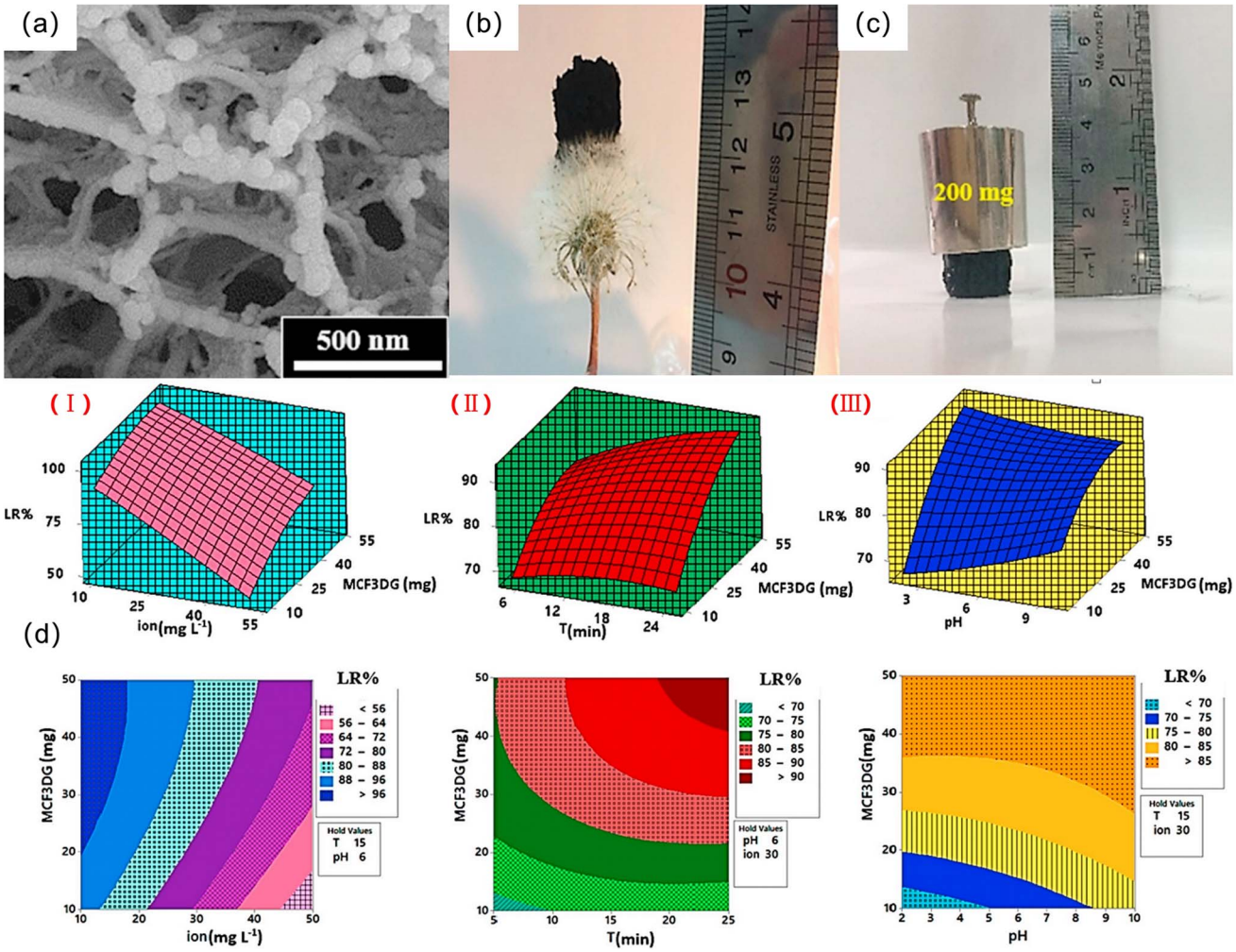

Fig. 10 (a) FE-SEM images of the cross-section of MCF3DG, (b and c) photographs of a lightweight and strong MCF3DG supporting weight, (d) the combined influence of the lead ion concentration and adsorbent dosage (MCF3DG) (i); the combined influence of the adsorbent dosage and contact time (ii); the combined influence of the adsorbent dosage and solution pH (iii) on lead ion removal efficiency.

prepared adsorbent was magnetic, which was beneficial to the separation of substances in water (Fig. 9b). Cheraghipour *et al.* synthesized chitosan-conjugated magnetite nanobiocomposites (CH-MNP-CA).[119] One of the notable advantages of this nanobiocomposite is its chemical conjugation, which does not have the weakness of the ultimate chitosan detachment of a physical bond and makes it easy for magnetic separation and does not produce secondary waste. At the same time, the nanoadsorbent also exhibited excellent renewability and reusability up to at least five cycles (Fig. 9c). Eivazzadeh-Keihan *et al.* designed a magnetic guanidinylated chitosan nanobiocomposite (MGC).[120] Compared with chitosan and magnetic chitosan, the material showed a better adsorption effect of heavy metal ions (the adsorption rates of Cu^{2+} and Pb^{2+} were 100% and 98.64%, respectively) (Fig. 9d) and can also be used for extracorporeal hyperthermia of cancer. After the *in situ* preparation of Fe_3O_4 magnetic cores to form MGC, the morphology of guanidyl chitosan changed greatly. The FE-SEM image of guanidyl chitosan is bar-shaped (Fig. 9e), while MGC has uniform and almost identical spherical morphological features, and the average size is between 30 nm and 34 nm (Fig. 9f).

In addition to the two types mentioned above, there are also studies that choose to use chitosan and other magnetic substances (such as $CoFe_2O_4$, $NiFe_2O_4$, *etc.*) to synthesize magnetic chitosan adsorption materials. Wu *et al.* synthesized a phosphorylated magnetic chitosan composite material (P-MCS).[121] With the increase in pH value, the adsorption of metal ions increases. The high adsorption capacity of Pb(II) on P-MCS is mainly due to coordination with the phosphonate group.[130] Nasiri *et al.* synthesized a novel magnetic three-dimensional graphene/chitosan/nickel ferrite nanocomposite (MCF3DG).[124] MCF3DG has a honeycomb-like 3D porous structure, and the $NiFe_2O_4$ nanoparticles are spherical due to magnetic attraction and attach to the surface of the material (Fig. 10a). The as-prepared nanocomposites are light in weight and exhibit good strength and weight resistance (Fig. 10b and c). MCF3DG has a good magnetic response with a saturation magnetization of approximately 11 emu g^{-1}. Based on plotting two-dimensional (2D) contour maps and three-dimensional

Table 5 The adsorption capacity of magnetic chitosan and its derivatives for Cr(VI)[a]

Adsorbent	Ion concentration ($mg\ L^{-1}$)	BET surface area ($m^2\ g^{-1}$)	Adsorption capacity of Cr(VI) ($mg\ g^{-1}$)	pH; temp (°C)	Kinetic model	Isotherm model	Cycles	Advantages	Reference
MC	—	—	—	5.32; 30	Pseudofirst-order	Langmuir	10	Nanoscale, large surface area	135
Fe(III)-CBs	5.0	—	166.3	6; 25	Pseudofirst-order	Langmuir-Freundlich	5	Reductive adsorption, small average diameter, easy separation and regeneration	136
ECSBNC	100	—	83.33	3; —	Pseudosecond-order	Langmuir	—	Spontaneous and endothermic adsorption process	95
MMMs	20	—	38.91	2; 30	Pseudofirst-order	Langmuir	5	High recovery and excellent reusability	137
DMCPs	200	—	153.85	3; 30	Pseudosecond-order	Langmuir	5	Wide pH range adsorption, easy separation and good reusability	138
Fe_3O_4/SiO_2/CS-TETA	150	131.4	254.6	2.5; 25	Pseudosecond-order	Langmuir	5	High adsorption capacity, fast adsorption rate and good reuse characteristics	139
VMCP	500	—	344.83	—; 25	Pseudosecond-order	Langmuir	5	Excellent removal performance	140
0.5-CLCh/MWCNT/Fe-10	100	70.90	449.30	4; 25	Pseudosecond-order	Langmuir	10	High reuse rate, wide removal pH range, good removal effect	141

[a] Abbreviations: MC: chitosan (90% deacetylation) coated with magnetic adsorbent; Fe(III)-CBs: Fe(III)-crosslinked chitosan beads; ECSBNC: epichlorohydrin crosslinked chitosan Schiff base-Fe_3O_4 nanocomposite; MMMs: mixed matrix membranes; DMCPs: poly([2-(methacryloxy)ethyl] trimethylammonium chloride)-modified magnetic chitosan particles; Fe_3O_4/SiO_2/CS-TETA: triethylenetetramine-modified hollow Fe_3O_4/SiO_2/chitosan magnetic nanocomposites; VMCP: poly(4-vinylpyridine)-decorated magnetic chitosan biopolymer; 0.5-CLCh/MWCNT/Fe-10: multiwalled carbon nanotubes (MWCNTs) doped with magnetic iron oxide and deposited in crosslinked chitosan (CLCh).

(3D) response surface maps (Fig. 10d), the effects of experimental variables (amount of absorbent, lead ion concentration, contact time, and pH) on lead ion removal efficiency were obtained. With increasing MCF3DG dosage, the initial Pb(II) ion concentration decreased, the contact time increased, the pH increased, and the removal efficiency of Pb(II) increased, which could exceed 98%, showing excellent adsorption capacity.

4.3 Adsorption of Cr

Cr exists in the form of trivalent chromium (Cr(III)) and hexavalent chromium (Cr(VI)) under natural conditions.[131] Chromium is one of the trace elements necessary for life, but chromium is toxic, and excessive use will pollute the environment.[132] Cr(VI) is more toxic than Cr(III), and it is a carcinogen that is easily absorbed by the body and accumulates in the body.[133] The World Health Organization stipulates that the maximum allowable concentration of Cr^{6+} in drinking water is 50 ppb,[134] but chromium exists in actual industrial wastewater and natural water, so chromium ion treatment is required before water supply.

Table 5 summarizes many examples of magnetic chitosan materials for Cr(VI) adsorption. It can be seen that MC and 0.5-CLCh/MWCNT/Fe-10 have better recyclability and the best adsorption performance, and Fe_3O_4/SiO_2/CS-TETA has a larger specific surface area. For the adsorption process of Cr, most of them conform to the Langmuir isothermal adsorption line. In terms of adsorption kinetics, some of the materials conform to pseudofirst-order kinetics, and the rest conform to pseudosecond-order kinetics, with no large bias. It can be seen from Fig. 11a that for the modification of chromium ion adsorption materials, the effect of reduction adsorption is indeed better than that of group modification, which may be related to the immobilization of Cr(III) after reduction. Most of the studies on Cr on magnetic chitosan materials are aimed at the adsorption of Cr^{6+}, and we believe that more efficient Cr(III) adsorption of magnetic chitosan and its derivatives remains to be developed.

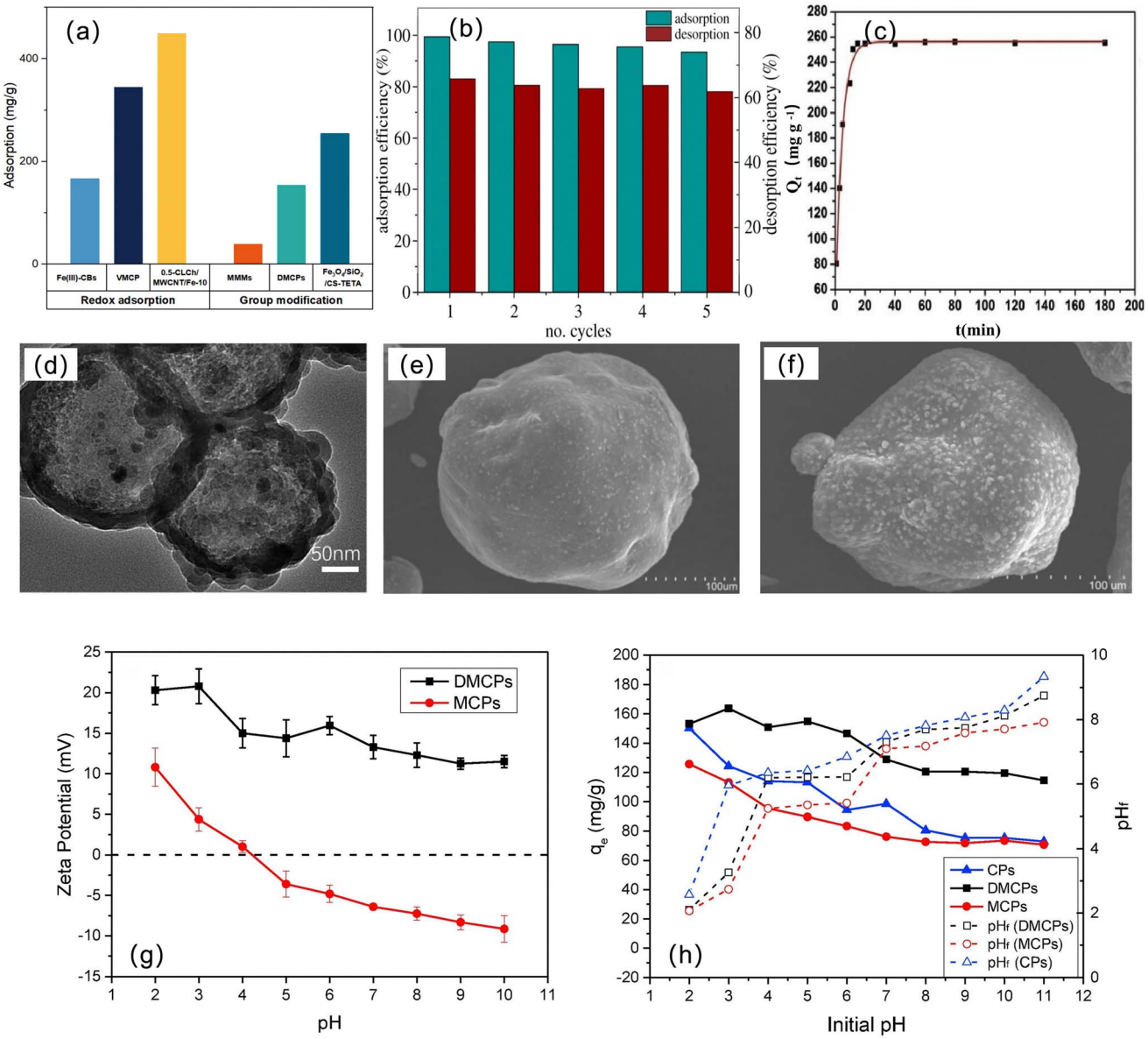

Fig. 11 (a) Adsorption capacity diagram of magnetic chitosan materials modified by different methods of Cr(VI), (b) Cr(VI) adsorption–desorption behaviors on Fe(III)-CBs, (c) adsorption kinetics of Cr(VI) ions. (d) TEM images of hollow Fe_3O_4/SiO_2/CS-TETA nanocomposites, (e) SEM images of MCPs, (f) SEM images of DMCPs, (g) ZP–pH profiles of the magnetic adsorbents, and (h) effect of pH on the adsorption capacity of Cr(VI).

Due to the high mobility of Cr(VI), Cr(VI) adsorbed on the adsorbent surface can be released into the solution again and cannot reduce the toxicity caused by Cr(VI).[142] Therefore, many studies on the reduction adsorption of Cr(VI) by magnetic chitosan not only have the advantages of adsorption but also realize the detoxification of Cr(VI) and the immobilization of Cr(III).[143] Wu *et al.* synthesized Fe(III)-crosslinked chitosan beads (Fe(III)-CBs).[136] The adsorption process fit the Langmuir–Freundlich isotherm best, the adsorption capacity was determined to be 166.3 mg g^{-1}, and Cr(VI) adsorbed on the beads was reduced to Cr(III). After 5 adsorption/desorption/regeneration cycles, the initial adsorption capacity remained above 93% (Fig. 11b). Zheng *et al.* prepared a poly(4-vinylpyridine)-decorated magnetic chitosan biopolymer (VMCP) as an absorbent and reductant to remove Cr(VI).[140] The kinetic and isothermal experiments show that the Cr(VI) removal system is well described by the pseudosecond-order and Langmuir models, and VMCP has rapid separation and satisfactory regeneration ability. After 5 adsorption–desorption cycles, the adsorption capacity was still as high as 246.0 mg g^{-1}.

However, magnetic chitosan materials will have magnetic particles occupying the surface of chitosan, resulting in a decrease in effective adsorption sites, such as when $-NH_2$ adsorption is weakened. Therefore, some studies have been modified by group modification, such as the introduction of amino group-rich substances, and obtained a better adsorption effect. Wang *et al.* prepared a triethylenetetramine ()-modified

hollow Fe_3O_4/SiO_2/chitosan magnetic nanocomposites (Fe_3O_4/SiO_2/CS-TETA).[139] The material reached adsorption equilibrium within 15 minutes, and the adsorption capacity reached 254.6 mg g^{-1} (Fig. 11c), showing the characteristics of fast adsorption speed and high adsorption capacity, due to the hollow structure of the prepared material (Fig. 11d), increasing the adsorption sites of metal ions on the material.[144] Zheng *et al.* synthesized a new type of adsorbent: poly([2-(methacryloxy) ethyl]trimethylammonium chloride) (PDMC)-modified magnetic chitosan particles (DMCPs).[138] PDMC contains abundant quaternary ammonium salt groups, and the introduction of PDMC significantly improves the adsorption performance of magnetic chitosan.[145] The surface of DMCPs is rougher than that of magnetic chitosan particles (MCPs) and possesses more active sites (Fig. 11e and f). In addition, it can be seen from Fig. 11g and h that the zeta potential of DMCPs is positive in the entire pH range tested, while the zeta potential of MCPs will decrease to below 0, so DMCPs have a wider pH range and better adsorption performance for anionic pollutants than MCPs.

4.4 Adsorption of other metal ions

In addition to the abovementioned metal ions, magnetic chitosan materials have also been studied and applied in the

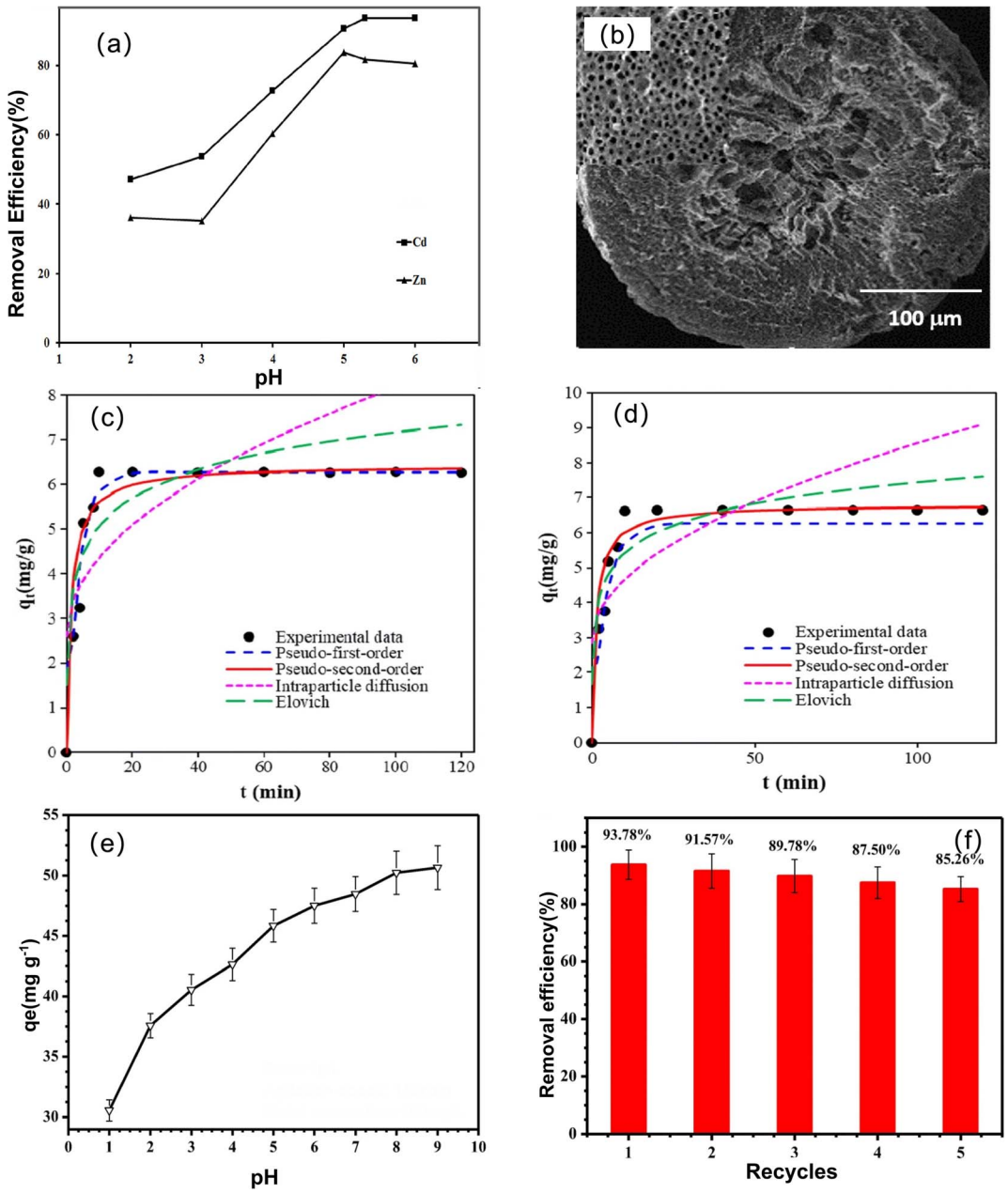

Fig. 12 (a) Effect of pH on the removal of metal ions onto EDTA-M-Cs, (b) SEM micrographs for the Ch/g-HNTs@ZnγM composite, the experimental and kinetic plots of (c) V(v) and (d) Pd(ii) adsorption on Fe_3O_4-CSN, (e) effects of pH on adsorption behavior of Co(ii), and (f) adsorption-desorption recycles for the removal of Co(ii).

adsorption of other metal ions, such as Zn^{2+}, Pd^{2+}, Cd^{2+}, Hg^{2+}, Mn^{2+}, and Fe^{3+}.

Fatemeh *et al.* developed a magnetic chitosan/Al_2O_3/Fe_3O_4 nanocomposite (EDTA-M-Cs) to remove Cd(II) and Zn(II) metal ions.[146] EDTA functionalization increases the adsorption capacity of Cd and Zn ions by ~5.6 and ~14.3 times, and the removal rates are 99.98 and 83.81%, respectively. The adsorption of Cd(II) and Zn(II) ions by EDTA-M-Cs is highly pH-dependent (Fig. 12a). Mubarak *et al.* prepared a chitosan/grafted halloysitenanotubes@Znγmagnetite quaternary nanocomposite (Ch/g-HNTs@ZnγM).[147] Magnetic iron exists in the internal structure of the Ch/g-HNTs@ZnγM material, and gaps and holes with high electron density are clearly exhibited on its surface (Fig. 12b). The adsorption of Mn(II) decreased with increasing ion concentration, while Fe showed the opposite trend, and the maximum adsorption and removal rates of Fe(III) and Mn(II) ions were 99.06% and 87.1%, respectively. Rahmi *et al.* prepared magnetic chitosan beads and applied them to remove Hg(II) and Cd(II).[148] The adsorption capacities of magnetic chitosan beads for Hg(II) and Cd(II) are 0.4 and 3.04 mg g^{-1}, respectively, which are higher than those of pure chitosan. Maryam *et al.* synthesized magnetic chitosan nanoparticles (Fe_3O_4-CSN)[149] for the removal of vanadium (V(v)) and palladium (Pd(II)) ions. The removal efficiencies of V(v) and Pd(II) ions are 99.9% and 92.3%, respectively, and both ions conform to pseudosecond-order kinetics (Fig. 12c and d), which is a combination of physical adsorption and chemical adsorption. Thermodynamic studies show that the adsorption process is exothermic and spontaneous.

Co, Ni, rare earth elements, *etc.*, are strategic and scarce resources with important industrial applications. Therefore, the adsorption and recovery of these metal ions has been extensively explored by researchers. Li *et al.* prepared a new type of amidoxime-based magnetic adsorbent.[150] Under the optimal conditions, the maximum adsorption efficiency for Ni(II) ions is 32.68 mg g^{-1}. Dong *et al.* synthesized magnetic phosphorylated chitosan composite (P-MCS).[151] The amount of Co(II) adsorption increases significantly with increasing pH value(Fig. 12e). The maximum adsorption capacity of Co(II) is 46.1 mg g^{-1}, and it still retains 85.26% of the adsorption capacity after five cycles (Fig. 12f).

Based on the above content, we can conclude that magnetic chitosan materials have been widely used in the field of metal ions in wastewater, and there have been many studies on further modification by introducing groups, strengthening the structure of chitosan, and synergistic effects of composite substances to further enhance the adsorption performance of magnetic chitosan materials. At the same time, its adsorption performance varies with the initial concentration of metal ions,

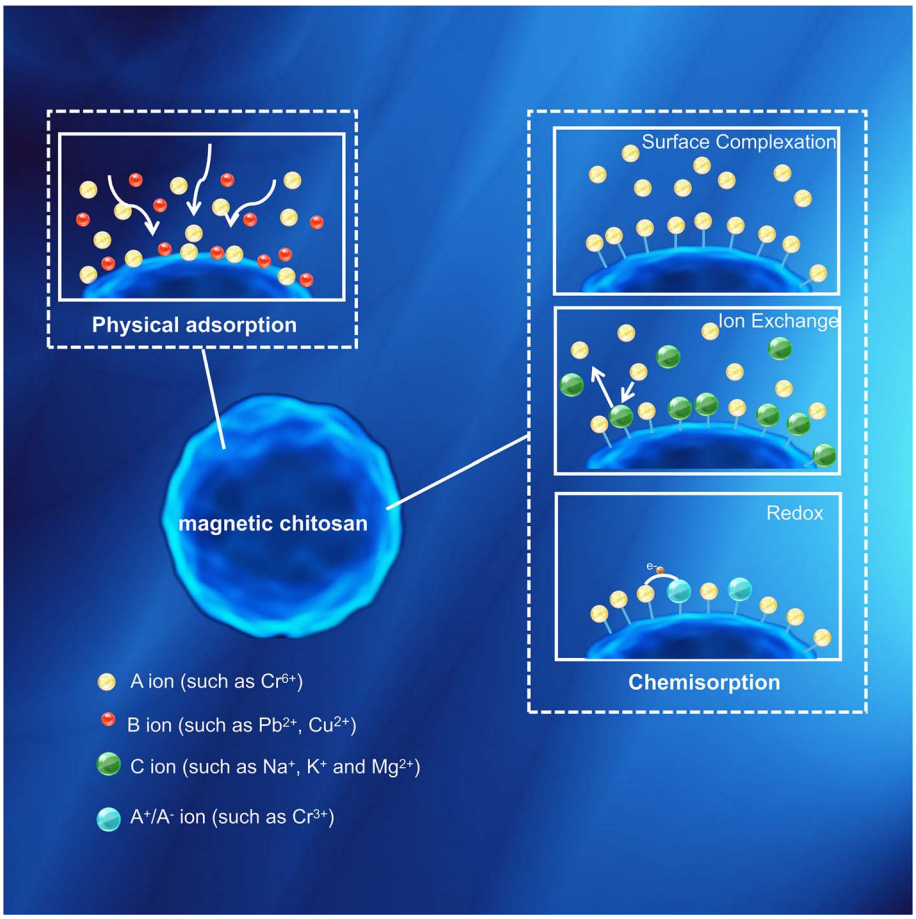

Fig. 13 Summary of the magnetic chitosan adsorption mechanism.

the pH value of the solution, the reaction temperature, the contact time and the chemical properties of different metal ions. It is necessary to consider its reusability and desorption reagents in practical applications.

5. Adsorption mechanism

The type of surface functional groups and the adsorption environment will affect the adsorption effect, so the main adsorption mechanism of heavy metals on different magnetic chitosan adsorption materials will be different. According to the existing research results, the adsorption mechanism of heavy metal ions on magnetic chitosan can be divided into two categories, including physical adsorption and chemical adsorption (Fig. 13).

5.1 Physical adsorption

Physical adsorption is a mechanism that occurs through weak electrostatic interactions such as van der Waals forces.[152] Since physical adsorption is mainly caused by intermolecular forces, the adsorption affinity is often weak. Therefore, the adsorption process may be reversible. At the same time, the strength of electrostatic interactions is closely related to the pH value of the solution, the valence state of heavy metals, the ionic radius and other factors. For example, heavy metal ions exist in different forms under different pH conditions. Hachem *et al.*[153] studied the adsorption of Pb(II). At low pH, the Pb species are mainly Pb^{2+} and $PbNO^{3+}$, and there is competition between H^+ and Pb^{2+}. As the pH value increases, the positive charge density at the surface position of the adsorbent decreases, so the ability of the adsorbent to adsorb Pb^{2+} ions increases, but when the pH is higher than 6, the Pb species will become $Pb(OH)_2$, which reduces the adsorption ability.[154] Zheng *et al.* studied the adsorption of Cr(VI).[155] At pH 2.0–6.4, the main Cr(VI) substances are $HCrO_4^-$ and $Cr_2O_7^{2-}$, while at pH 6.4 or higher, the main ionic form of Cr(VI) is CrO_4^{2-} and the high adsorption capacity of Cr(VI) ions occurs at lower pH. Therefore, it can be concluded that the adsorption properties of Pb(II) and Cr(VI) show an opposite trend with the change in pH (Fig. 14a), which is due to the electrostatic interaction between the charges of the ions and the protonated amino and hydroxyl groups.

5.2 Chemisorption

Chemisorption often occurs through three separate forms, including ion exchange, surface complexation, redox, or a combination of these steps.

In the case of ion exchange, when there are exchangeable ions (such as Na^+, K^+ and Mg^{2+}) on the magnetic chitosan surface through direct or indirect coupling, the heavy metal ions in the aqueous solution are exchanged with these

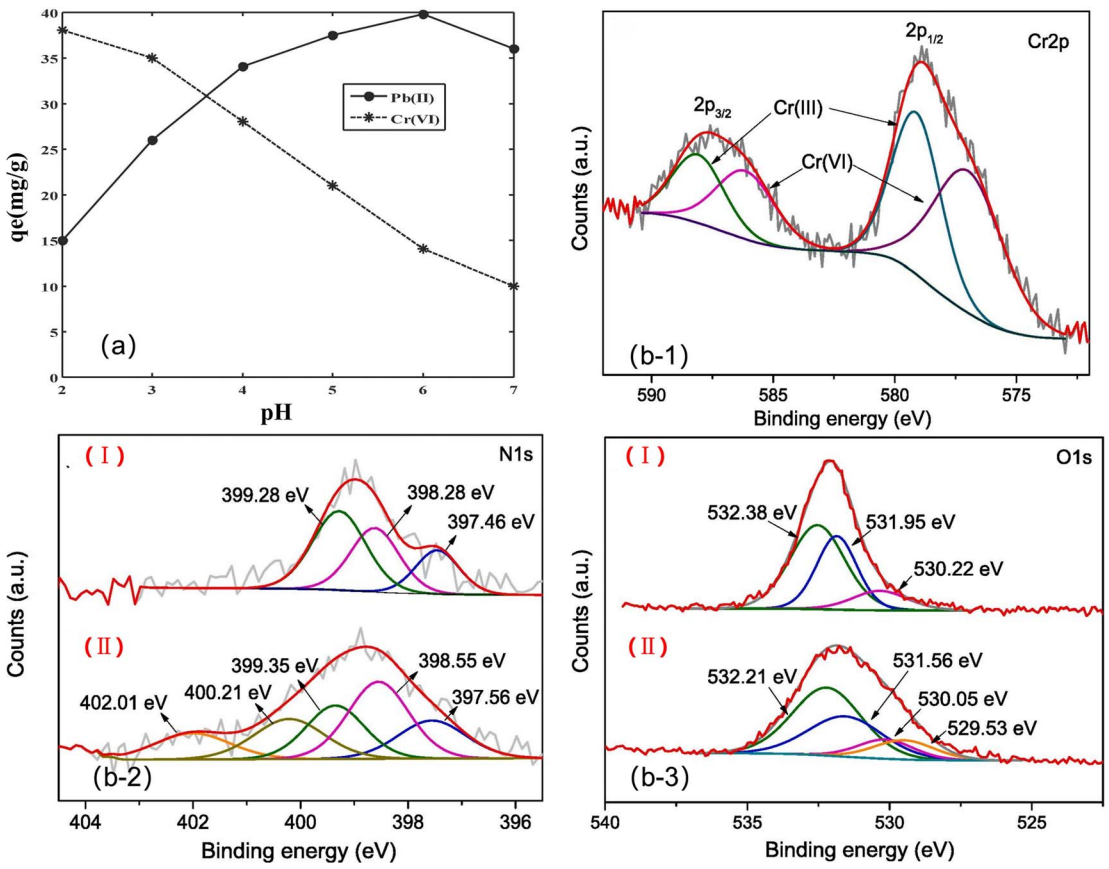

Fig. 14 (a) Effect of pH on the metal ions removal using the PVA/chitosan/a-Fe_3O_4-2 nanofibrous membrane,[137] (b-1) Cr 2p XPS spectra of Cr-loaded VMCP; (b-2) N 1s spectra before (i) and after adsorption (ii); (b-3) O 1s spectra before (i) and after adsorption (ii).

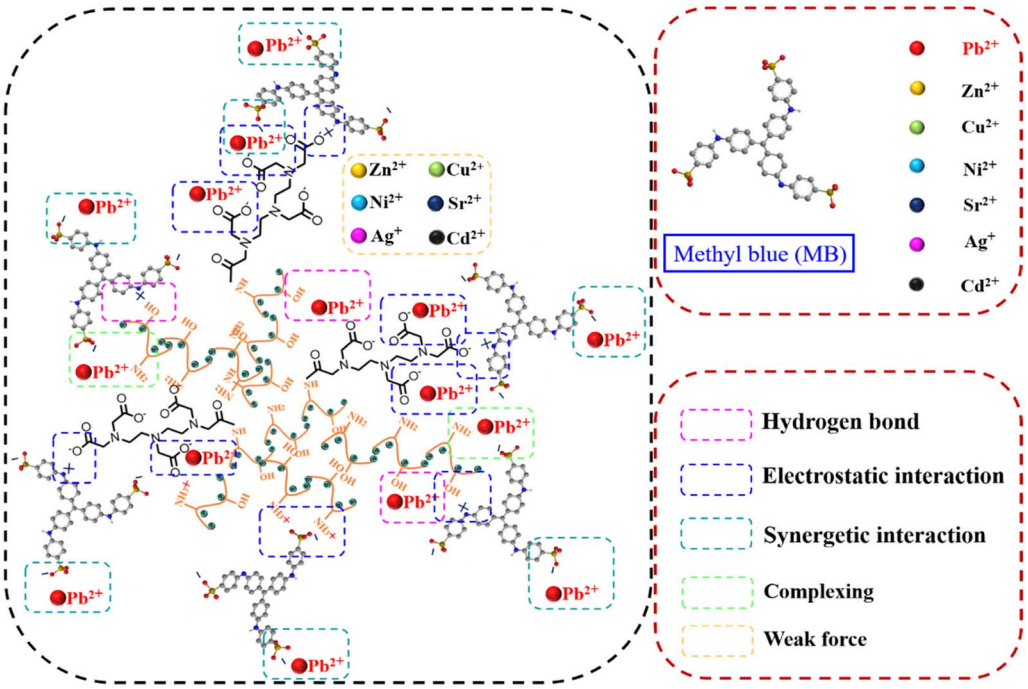

Fig. 15 Proposed adsorption mechanism using FFO@Sil@Chi-DTPA to capture MB and Pb(II) simultaneously.

exchangeable ions to remove heavy metal ions. Zhang *et al.*[156] reported that ion exchange is one of the adsorption mechanisms for Cr(VI) removal by Fe_3O_4-CS/PDAC.

Surface complexation depends on the interaction between surface functional groups and heavy metal ions. Positively or negatively charged groups on the surface of magnetic chitosan, such as hydroxyl, carboxyl, ester or amine groups, attract oppositely charged ions in solution and form complexes through chemical bonding on the surface. For example, Ping *et al.*[157] reported that –NH/–NH_2, O=C–O– and C–O–H functional groups in Fe_3O_4-ATP/EDTA/CS play important roles in the adsorption process of heavy metal ions.

Redox affects the chemical behavior of elements by changing their existing forms, mainly occurring in heavy metals with variable valence. Cai *et al.*[158] studied the adsorption mechanism and found that under acidic conditions, strongly oxidizing Cr(VI) can be reduced to Cr(III) through the reducing –OH group in the adsorbent. According to FTIR and XPS spectra, Zheng *et al.*[140] explained that the main adsorption mechanism of the prepared magnetic chitosan biopolymer (VMCP) was that Cr(VI) was adsorbed on the positively charged VMCP surface and Cr(VI) was reduced to Cr(III), followed by the coordination between Cr(III) and N atoms (Fig. 14b).

5.3 Collaborative adsorption

At the same time, there is a process of physical adsorption and chemical adsorption. Song *et al.*[159] reported the abundant –NH, –OH, and –SH groups in Cyshtcc-Fe_3O_4, which can perform ion exchange and surface complexation of various heavy metal ions. The physical adsorption electrostatic interaction also improves the adsorption capacity of the composites. Huang *et al.* investigated the adsorption mechanism for the simultaneous capture of methylene blue (MB) and Pb(II) by the FFO@Sil@Chi-DTPA material in a binary pollution system[122] (Fig. 15). Pb(II) binds to the carboxyl group by electrostatic attraction, binds to the hydroxyl group by hydrogen bonding, and coordinates with amino groups through complexation; the MB adsorbed onto the adsorbent surface can create new specific sites (the sulfonic acid groups in MB molecules) to enhance Pb(II) adsorption. Additionally, the Pb(II) adsorbed onto the adsorbent surface can act as the cation bridge and enhance the adsorption of MB *via* electrostatic attraction.

Based on Tables 3–5, most of the research indicates that the adsorption behavior of Cu(II), Pb(II) and Cr(VI) can be well described by the Langmuir model, and a few fit the Freundlich model. Therefore, the results indicate that the magnetic chitosan has a uniform distribution of surface sites active for metal adsorption. At the same time, it is also very suitable for the pseudosecondary model, indicating that chemical adsorption is the rate determining step of the adsorption process.

6. Conclusions and future perspectives

In recent years, the problem of water pollution has become increasingly serious. It is urgent to develop green and sustainable water treatment technology. Magnetic chitosan microspheres have the advantages of low cost, high adsorption rate, good biological activity, and easy separation and regeneration. This is undoubtedly one of the important directions of water treatment in the future. Although magnetic chitosan has been widely studied and modified to enhance its stability and

adsorption performance, the adsorption performance of magnetic chitosan for some ions is still not ideal, and the use of toxic chemical reagents in the preparation process is not green enough. Therefore, in future research, it is necessary to develop greener ways to prepare materials and increase the recycling of materials to synthesize green and environmentally friendly adsorbents, such as replacing toxic crosslinking agents with natural products and green synthesis of magnetic cores. To further improve the adsorption performance, we believe that it may be possible to combine chitosan with biological substances, such as the immobilization of biological enzymes on the surface of magnetic chitosan to accelerate the decomposition of pollutants by catalytic degradation of enzymes.

At the same time, in order to realize the practical application of adsorbents, it should be noted that there are many kinds of pollutants in the actual sewage treatment. At present, most studies are aimed at the adsorption of single-component heavy metal ions. Therefore, in the future, it is possible to explore and improve the highly selective adsorption of adsorption materials on multi-component mixed pollutants.

Author contributions

All authors listed have significantly contributed to the development and the writing of this article. Ke Wang and Fanbing Zhang contributed to data collection, analysis and drafting the manuscript. Kexin Xu and Yuju Che contributed to pictures collection and typesetting. Mingying Qi and Cui Song contributed to the conception of the study and helped perform the analysis with constructive discussions. After the first draft is completed, all authors read, discuss, revise and finalize the manuscript.

Conflicts of interest

The authors have no relevant financial or non-financial interests to disclose.

Acknowledgements

The authors acknowledge supports from the National Natural Science Foundation of China (4217030124), Natural Science Foundation of Shandong Province (ZR2021MB052, ZR2020MB140), and Shandong University-Weihai Research Institute of Industry Technology Research Projects (0004202107020002).

References

1 J. Ma, S. Zuo-Jiang, Y. He, Q. Sun, Y. Wang, W. Liu, S. Sun and K. Chen, *R. Soc. Open Sci.*, 2016, **3**, 160524.
2 N. Vatanpour, J. Feizy, H. H. Talouki, Z. Es'haghi, L. Scesi and A. M. Malvandi, *Chemosphere*, 2020, **245**, 125639.
3 K. Rana, M. Kumar and A. Kumar, *Water, Air, Soil Pollut.*, 2020, **231**, 450.
4 N. Adimalla, J. Chen and H. Qian, *Ecotoxicol. Environ. Saf.*, 2020, **194**, 110406.
5 A. Kumar, M. Cabral-Pinto, M. Kumar and P. A. Dinis, *Appl. Sci.*, 2020, **10**, 7078.
6 L. M. Liao, M. C. Friesen, Y.-B. Xiang, H. Cai, D.-H. Koh, B.-T. Ji, G. Yang, H.-L. Li, S. J. Locke, N. Rothman, W. Zheng, Y.-T. Gao, X.-O. Shu and M. P. Purdue, *Environ. Health Perspect.*, 2016, **124**, 97–103.
7 P. Mitra, S. Sharma, P. Purohit and P. Sharma, *Crit. Rev. Clin. Lab. Sci.*, 2017, **54**, 506–528.
8 D. C. Ong, M. D. G. de Luna, S. M. B. Pingul-Ong and C. C. Kan, *J. Environ. Manage.*, 2018, **223**, 723–730.
9 M. L. F. A. De Castro, M. L. B. Abad, D. A. G. Sumalinog, R. R. M. Abarca, P. Paoprasert and M. D. G. de Luna, *Sustainable Environ. Res.*, 2018, **28**, 197–205.
10 S. B. Tumampos, B. M. B. Ensano, S. M. B. Pingul-Ong, D. C. Ong, C. C. Kan, J. J. Yee and M. D. G. de Luna, *Int. J. Environ. Res. Public Health*, 2021, **18**, 3050.
11 I. O. Saheed, W. D. Oh and F. B. M. Suah, *J. Hazard. Mater.*, 2021, **408**, 124889.
12 U. Habiba, T. C. Joo, T. A. Siddique, A. Salleh, B. C. Ang and A. M. Afifi, *Int. J. Biol. Macromol.*, 2017, **104**, 1133–1142.
13 T. V. J. Charpentier, A. Neville, J. L. Lanigan, R. Barker, M. J. Smith and T. Richardson, *ACS Omega*, 2016, **1**, 77–83.
14 Y. Z. Xiao, H. F. Liang and Z. C. Wang, *Mater. Res. Bull.*, 2013, **48**, 3910–3915.
15 G. D. Briao, J. R. de Andrade, M. G. C. da Silva and M. G. A. Vieira, *Environ. Chem. Lett.*, 2020, **18**, 1145–1168.
16 V. R. Shaumbwa, D. G. Liu, B. Archer, J. L. Li and F. Su, *J. Appl. Polym. Sci.*, 2021, **138**, e51241.
17 G. Michailidou, I. Koumentakou, E. V. Liakos, M. Lazaridou, D. A. Lambropoulou, D. N. Bikiaris and G. Z. Kyzas, *Polymers*, 2021, **13**, 3137.
18 S. X. Liu, B. Yu, S. Wang, Y. Q. Shen and H. L. Cong, *Adv. Colloid Interface Sci.*, 2020, **281**, 102165.
19 L. S. Ganapathe, M. A. Mohamed, R. M. Yunus and D. D. Berhanuddin, *Magnetochemistry*, 2020, **6**, 68.
20 J. Tong and L. G. Chen, *Anal. Lett.*, 2013, **46**, 2635–2656.
21 V. R. Shaumbwa, D. G. Liu, B. Archer, J. L. Li and F. Su, *J. Appl. Polym. Sci.*, 2021, **138**, e51241.
22 A. G. Perez, E. Gonzalez-Martinez, C. R. D. Aguila, D. A. Gonzalez-Martinez, G. G. Ruiz, A. G. Artalejo and H. Yee-Madeira, *Colloids Surf., A*, 2020, **591**, 124500.
23 G.-T. Zhu, X.-L. Hu, S. He, X.-M. He, S.-K. Zhu and Y.-Q. Feng, *J. Chromatogr. A*, 2018, **1564**, 42–50.
24 F. Zhao, B. Y. Yu, Z. G. Yue, T. Wang, M. Wen, Z. B. Liu and C. S. Zhao, *J. Hazard. Mater.*, 2007, **147**, 67–73.
25 N. H. Shalaby, E. M. M. Ewais, R. M. Elsaadany and A. Ahmed, *Egypt. J. Pet.*, 2017, **26**, 661–668.
26 H. El Knidri, R. Belaabed, A. Addaou, A. Laajeb and A. Lahsini, *Int. J. Biol. Macromol.*, 2018, **120**, 1181–1189.
27 Y. L. Nunes, F. L. de Menezes, I. G. de Sousa, A. L. Gama Cavalcante, F. T. Tavares Cavalcante, K. d. S. Moreira, A. L. Barros de Oliveira, G. F. Mota, J. E. da Silva Souza, I. R. de Aguiar Falcao, T. G. Rocha, R. B. Rodrigues Valerio, P. B. Almeida Fechine, M. C. Martins de Souza and J. C. S. dos Santos, *Int. J. Biol. Macromol.*, 2021, **181**, 1124–1170.

28 A. Popa, A. Visa, B. Maranescu, I. Hulka and L. Lupa, *Materials*, 2021, **14**, 7894.
29 W. Wu, Q. He and C. Jiang, *Nanoscale Res. Lett.*, 2008, **3**, 397–415.
30 A. Hiroki, H. T. Tran, N. Nagasawa, T. Yagi and M. Tamada, *Radiat. Phys. Chem.*, 2009, **78**, 1076–1080.
31 B. H. Hameed and M. I. El-Khaiary, *J. Hazard. Mater.*, 2008, **157**, 344–351.
32 S. Liu, B. Yu, S. Wang, Y. Shen and H. Cong, *Adv. Colloid Interface Sci.*, 2020, **281**, 102165.
33 P. G. Krishnan, S. Muthukumaran and V. Raja, *J. Lumin.*, 2021, **238**, 118258.
34 U. A. Agu, M. I. Oliva, S. G. Marchetti, A. C. Heredia, S. G. Casuscelli and M. E. Crivello, *J. Magn. Magn. Mater.*, 2014, **369**, 249–259.
35 J. Sahadevan, R. Sojiya, N. Padmanathan, K. Kulathuraan, M. G. Shalini, P. Sivaprakash and S. E. Muthu, *Magnetic property of Fe_2O_3 and Fe_3O_4 nanoparticle prepared by solvothermal process*, Tiruchirappalli, India, 2021.
36 M. Imran, A. M. Affandi, M. M. Alam, A. Khan and A. I. Khan, *Nanotechnology*, 2021, **32**, 422001.
37 J. A. Flood-Garibay and M. A. Mendez-Rojas, *Colloids Surf., A*, 2021, **615**, 126236.
38 Z. Chen, X. Song, W. W. M. Soh, Y. Wen, J. Zhu, M. Zhang and J. Li, *Gels*, 2021, **7**, 201.
39 L. Shen, B. Li and Y. Qiao, *Materials*, 2018, **11**, 324.
40 S. Rezayati, F. Kalantari, A. Ramazani, S. Sajjadifar, H. Aghahosseini and A. Rezaei, *Inorg. Chem.*, 2022, **61**, 992–1010.
41 S. J. Olusegun, G. L. S. Rodrigues, E. T. F. Freitas, L. R. S. Lara, W. R. Rocha and N. D. S. Mohallem, *J. Hazard. Mater.*, 2019, **380**, 120872.
42 L. Zhang, X. Zhu, S. Zheng and H. Sun, *Biochem. Eng. J.*, 2009, **46**, 83–87.
43 D.-M. Liu, C. Dong, J. Zhong, S. Ren, Y. Chen and T. Qiu, *Carbohydr. Polym.*, 2020, **245**, 116572.
44 J. Jumadi, A. Kamari, N. A. Rahim, S. T. S. Wong, S. N. M. Yusoff, S. Ishak, M. M. Abdulrasool and S. Kumaran, *J. Phys.: Conf. Ser.*, 2019, **1397**, 012027–012028.
45 H. Zhao, J. Xu, W. Lan, T. Wang and G. Luo, *Chem. Eng. J.*, 2013, **229**, 82–89.
46 S. Ben Ayed, H. M. Sbihi, M. Azam, S. I. Al-Resayes, M. T. Ayadi and F. Ayari, *Desalin. Water Treat.*, 2021, **220**, 446–458.
47 Y. Xu, Y. Zhang, X. Song and H. Liu, *Funct. Mater. Lett.*, 2019, **12**, 1950019.
48 R. Hufschmid, H. Arami, R. M. Ferguson, M. Gonzales, E. Teeman, L. N. Brush, N. D. Browning and K. M. Krishnan, *Nanoscale*, 2015, **7**, 11142–11154.
49 M. Liu, X. Sun, Z. Liao, Y. Li, X. Qi, Y. Qian, H. Fenniri, P. Zhao and J. Shen, *Drug Delivery*, 2019, **26**, 732–743.
50 K. Zhang, X. Zhang, X. Zhao, X. Gai, W. An, G. Fang, A. Zhang and X. Chen, *J. Mater. Sci.: Mater. Electron.*, 2019, **30**, 17333–17341.
51 G. H. Du, Z. L. Liu, X. Xia, Q. Chu and S. M. Zhang, *J. Sol-Gel Sci. Technol.*, 2006, **39**, 285–291.
52 C.-H. Lu, G.-H. Chen, B. Yu, H.-L. Cong, L.-M. Kong and L. Guo, *Integr. Ferroelectr.*, 2017, **182**, 46–52.
53 Y. Jiang, W. Cai, W. Tu and M. Zhu, *J. Chem. Eng. Data*, 2019, **64**, 226–233.
54 I. Fatimah, E. Z. Pratiwi and W. P. Wicaksono, *Egypt. J. Aquat. Res.*, 2020, **46**, 35–40.
55 A. V. Ramesh, D. R. Devi, S. M. Botsa and K. Basavaiah, *J. Asian Ceram. Soc.*, 2018, **6**, 145–155.
56 A. Sebastian, A. Nangia and M. N. V. Prasad, *J. Cleaner Prod.*, 2018, **174**, 355–366.
57 E. C. Nnadozie and P. A. Ajibade, *Mater. Lett.*, 2020, **263**, 127145.
58 Y. C. Lopez and M. Antuch, *Curr. Opin. Green Sustainable Chem.*, 2020, **24**, 32–37.
59 M. Rahmayanti, A. N. Syakina, I. Fatimah and T. Sulistyaningsih, *Chem. Phys. Lett.*, 2022, **803**, 139834.
60 P. Senthilkumar, L. Surendran, B. Sudhagar, R. S. D. S. Kumar and G. Bupesh, *Mater. Res. Express*, 2019, **6**, 095405.
61 X. Li, K. Cui, Z. Guo, T. Yang, Y. Cao, Y. Xiang, H. Chen and M. Xi, *Chem. Eng. J.*, 2020, **379**, 122324.
62 X. Li, D. Zeng, P. Ke, G. Wang and D. Zhang, *RSC Adv.*, 2020, **10**, 7163–7169.
63 S. Vaewbundit and P. Siriphannon, *Soft Matter*, 2021, **17**, 6238–6247.
64 R. N. Queiroz, P. Prediger and M. G. A. Vieira, *J. Hazard. Mater.*, 2022, **422**, 126904.
65 R. N. Queiroz, T. d. F. Neves, M. G. C. da Silva, V. R. Mastelaro, M. G. A. Vieira and P. Prediger, *J. Cleaner Prod.*, 2022, **361**, 132244.
66 S. Liu, H. Ge, S. Cheng and Y. Zou, *Environ. Technol.*, 2020, **41**, 2109–2121.
67 A. Kalidason and T. Kuroiwa, *React. Funct. Polym.*, 2022, **173**, 105220.
68 I. Rahmi and I. Mustafa, *Microchem. J.*, 2019, **144**, 397–402.
69 S. Y. Nam and Y. M. Lee, *J. Membr. Sci.*, 1999, **157**, 63–71.
70 R. Huang, Q. Liu, J. Huo and B. Yang, *Arabian J. Chem.*, 2017, **10**, 24–32.
71 D. A. Sahbaz, A. Yakar and U. Gunduz, *Part. Sci. Technol.*, 2019, **37**, 728–736.
72 N. A. Abdelwahab and A. M. Ghoneim, *Mater. Sci. Eng., B*, 2018, **228**, 7–17.
73 X. Cai, J. Li, Y. Liu, X. Hu, X. Tan, S. Liu, H. Wang, Y. Gu and L. Luo, *Int. J. Environ. Res. Public Health*, 2020, **17**, 6.
74 M. H. Karimi, G. R. Mandavinia, B. Massoumi, A. Baghban and M. Saraei, *Int. J. Biol. Macromol.*, 2018, **113**, 361–375.
75 A. Reghioua, D. Barkat, A. H. Jawad, A. S. Abdulhameed and M. R. Khan, *Sustainable Chem. Pharm.*, 2021, **20**, 100379.
76 B. Liu, X. Chen, H. Zheng, Y. Wang, Y. Sun, C. Zhao and S. Zhang, *Carbohydr. Polym.*, 2018, **181**, 327–336.
77 H.-R. Kim, J.-W. Jang and J.-W. Park, *J. Hazard. Mater.*, 2016, **317**, 608–616.
78 P. Xu, M. Zheng, N. Chen, Z. Wu, N. Xu, J. Tang and Z. Teng, *J. Taiwan Inst. Chem. Eng.*, 2019, **104**, 210–218.
79 N. Ayawei, A. N. Ebelegi and D. Wankasi, *J. Chem.*, 2017, **2017**, 3039817.

80 M. Gholami, A. Jonidi-Jafari, M. Farzadkia, A. Esrafili, K. Godini and M. Shirzad-Siboni, *J. Environ. Manage.*, 2021, **294**, 112962.
81 D. A. Islam, A. Chakraborty, A. Roy, S. Das and H. Acharya, *ChemistrySelect*, 2018, **3**, 11816–11823.
82 Y. Zhao, X. Yang, P. Pan, J. Liu, Z. Yang, J. Wei, W. Xu, Q. Bao, H. Zhang and Z. Liao, *J. Electron. Mater.*, 2020, **49**, 6695–6705.
83 J. Rihel, *Nat. Chem. Biol.*, 2018, **14**, 638–639.
84 J. Kumar, K. B. Sathua and S. J. S. Flora, *Cell. Mol. Biol.*, 2019, **65**, 27–35.
85 D. M. Marques, V. Veroneze Junior, A. B. da Silva, J. R. Mantovani, P. C. Magalhaes and T. C. de Souza, *Water, Air, Soil Pollut.*, 2018, **229**, 138.
86 R. Viriyatum and C. E. Boyd, *J. World Aquacult. Soc.*, 2016, **47**, 667–675.
87 M. E. Peralta, R. Nistico, F. Franzoso, G. Magnacca, L. Fernandez, M. E. Parolo, E. Garcia Leon and L. Carlos, *Adsorption*, 2019, **25**, 1337–1347.
88 F. Xiao, J. Cheng, W. Cao, C. Yang, J. Chen and Z. Luo, *J. Colloid Interface Sci.*, 2019, **540**, 579–584.
89 H. Li, Z. Wang, X. Liu, F. Cui, C. Chen, Z. Zhang, J. Li, L. Song and R. Bai, *Chem. Phys. Lett.*, 2020, **755**, 137805.
90 M. A. M. Taguba, D. C. Ong, B. M. B. Ensano, C.-C. Kan, N. Grisdanurak, J.-J. Yee and M. D. G. de Luna, *Water*, 2021, **13**, 1662.
91 H.-C. Tao, S. Li, L.-J. Zhang, Y.-Z. Chen and L.-P. Deng, *Environ. Geochem. Health*, 2019, **41**, 297–308.
92 Z. Zhang, H. Li, J. Li, X. Li, Z. Wang, X. Liu and L. Zhang, *Chem. Phys. Lett.*, 2019, **731**, 136573.
93 L. Yang, Y. Peng, C. Qian, G. Xing, J. He, C. Zhao and B. Lai, *Chemosphere*, 2021, **263**, 128120.
94 C. Zhang, S. Liu, S. Li, Y. Tao, P. Wang, X. Ma and L. Chen, *Colloids Surf., A*, 2019, **581**, 123813.
95 S. M. Anush and B. Vishalakshi, *Int. J. Biol. Macromol.*, 2019, **133**, 1051–1062.
96 H. Hosseinzadeh and S. Ramin, *Int. J. Biol. Macromol.*, 2018, **113**, 859–868.
97 B. Chen, H. Zhao, S. Chen, F. Long, B. Huang, B. Yang and X. Pan, *Chem. Eng. J.*, 2019, **356**, 69–80.
98 X. Shen, J. Zhao, N. Bonet-Garcia, E. Villagrasa, A. Sole, X. Liao and C. Palet, *Int. J. Environ. Sci. Technol.*, 2022, **20**, 801–814.
99 M. R. Afrooz, B. K. Moghadas and S. Tamjidi, *J. Alloys Compd.*, 2022, **893**, 162321.
100 Z. Yu, X. Zhang and Y. Huang, *Ind. Eng. Chem. Res.*, 2013, **52**, 11956–11966.
101 H. Y. Zhu, R. Jiang, L. Xiao and G. M. Zeng, *Bioresour. Technol.*, 2010, **101**, 5063–5069.
102 A. Aisopou, I. Stoianov and N. J. D. Graham, *Water Res.*, 2012, **46**, 235–246.
103 J. Wang and C. Chen, *Biotechnol. Adv.*, 2006, **24**, 427–451.
104 Y. Wu, X. Qiu, S. Cao, J. Chen, X. Shi, Y. Du and H. Deng, *J. Colloid Interface Sci.*, 2019, **539**, 533–544.
105 A. Kumar, K. Amit, M. M. S. Cabral-Pinto, A. K. Chaturvedi, A. A. Shabnam, G. Subrahmanyam, R. Mondal, D. K. Gupta, S. K. Malyan, S. S. Kumar, S. A. Khan and K. K. Yadav, *Int. J. Environ. Res. Public Health*, 2020, **17**, 2179.
106 M. D. G. de Luna, L. M. Bellotindos, R. N. Asiao and M.-C. Lu, *Hydrometallurgy*, 2015, **155**, 6–12.
107 J. Cela, W. Bonilla and R. Urrutia-Goyes, *IOP Conference Series: Earth and Environmental Science*, 2021, **728**, 012006–012007.
108 J. Garcia-Leston, J. Mendez, E. Pasaro and B. Laffon, *Environ. Int.*, 2010, **36**, 623–636.
109 L. Lv, N. Chen, C. Feng, J. Zhang and M. Li, *RSC Adv.*, 2017, **7**, 27992–28000.
110 F. Bouhamed, Z. Elouear and J. Bouzid, *J. Taiwan Inst. Chem. Eng.*, 2012, **43**, 741–749.
111 S. Huang, C. Ma, Y. Liao, C. Min, P. Du, Y. Zhu and Y. Jiang, *React. Funct. Polym.*, 2016, **106**, 76–85.
112 S. Gunduz and S. Akman, *Food Chem.*, 2013, **141**, 2634–2638.
113 S. Shahraki and H. S. Delarami, *Carbohydr. Polym.*, 2018, **200**, 211–220.
114 C. Fan, K. Li, J. Li, D. Ying, Y. Wang and J. Jia, *J. Hazard. Mater.*, 2017, **326**, 211–220.
115 D. Hu, Z. Lian, H. Xian, R. Jiang, N. Wang, Y. Weng, X. Peng, S. Wang and X.-K. Ouyang, *Int. J. Biol. Macromol.*, 2020, **154**, 1537–1547.
116 B. Fahimirad, Y. Rangraz, A. Elhampour and F. Nemati, *Microchim. Acta*, 2018, **185**, 560.
117 M. F. Hamza, Y. Wei, H. I. Mira, A. A. H. Abdel-Rahman and E. Guibal, *Chem. Eng. J.*, 2019, **362**, 310–324.
118 Y. He, W. Xiao, G. Li, F. Yang, P. Wu, T. Yang, C. Chen and P. Ding, *Environ. Technol.*, 2019, **40**, 499–507.
119 E. Cheraghipour and M. Pakshir, *Chemosphere*, 2020, **260**, 127560.
120 R. Eivazzadeh-Keihan, F. Radinekiyan, S. Asgharnasl, A. Maleki and H. Bahreinizad, *J. Mater. Res. Technol.*, 2020, **9**, 12244–12259.
121 D. Wu, Y. Wang, Y. Li, Q. Wei, L. Hu, T. Yan, R. Feng, L. Yan and B. Du, *J. Mol. Liq.*, 2019, **277**, 181–188.
122 Y. Huang, H. Zheng, X. Hu, Y. Wu, X. Tang, Q. He and S. Peng, *J. Hazard. Mater.*, 2022, **422**, 126856.
123 D. P. Facchi, A. L. Cazetta, E. A. Canesin, V. C. Almeida, E. G. Bonafe, M. J. Kipper and A. F. Martins, *Chem. Eng. J.*, 2018, **337**, 595–608.
124 R. Nasiri, N. Arsalani and Y. Panahian, *J. Cleaner Prod.*, 2018, **201**, 507–515.
125 M. F. Hamza, M. M. Aly, A. A. H. Abdel-Rahman, S. Ramadan, H. Raslan, S. Wang, T. Vincent and E. Guibal, *Materials*, 2017, **10**, 539.
126 F. Zhao, E. Repo, M. Sillanpaa, Y. Meng, D. Yin and W. Z. Tang, *Ind. Eng. Chem. Res.*, 2015, **54**, 1271–1281.
127 A. A. Galhoum, A. A. Atia, M. G. Mahfouz, S. T. Abdel-Rehem, N. A. Gomaa, T. Vincent and E. Guibal, *J. Mater. Sci.*, 2015, **50**, 2832–2848.
128 M. F. Hamza, J.-C. Roux and E. Guibal, *Chem. Eng. J.*, 2018, **344**, 124–137.
129 E. A. Imam, I. E.-T. El-Sayed, M. G. Mahfouz, A. A. Tolba, T. Akashi, A. A. Galhoum and E. Guibal, *Chem. Eng. J.*, 2018, **352**, 1022–1034.

130 Y. Cai, C. Wu, Z. Liu, L. Zhang, L. Chen, J. Wang, X. Wang, S. Yang and S. Wang, *Environ. Sci.: Nano*, 2017, **4**, 1876–1886.
131 Y. Ma, W.-J. Liu, N. Zhang, Y.-S. Li, H. Jiang and G.-P. Sheng, *Bioresour. Technol.*, 2014, **169**, 403–408.
132 M. Imran, Z. U. H. Khan, M. M. Iqbal, J. Iqbal, N. S. Shah, S. Munawar, S. Ali, B. Murtaza, M. A. Naeem and M. Rizwan, *Environ. Pollut.*, 2020, **261**, 114231.
133 R. T. Kapoor, M. F. Bani Mfarrej, P. Alam, J. Rinklebe and P. Ahmad, *Environ. Pollut.*, 2022, **301**, 119044.
134 S. Azizi, I. Kamika and M. Tekere, *PLoS One*, 2016, **11**, e0155462.
135 T. Ravi and S. A. Jabasingh, *J. Appl. Polym. Sci.*, 2018, **135**, 45878.
136 Y. Wu, Y. Zhang, J. Qian, X. Xin, S. Hu, S. Zhang and J. Wei, *R. Soc. Open Sci.*, 2017, **4**, 170905.
137 S. Koushkbaghi, A. Zakialamdari, M. Pishnamazi, H. F. Ramandi, M. Aliabadi and M. Irani, *Chem. Eng. J.*, 2018, **337**, 169–182.
138 C. Zheng, H. Zheng, Y. Wang, Y. Wang, W. Qu, Q. An and Y. Liu, *Bioresour. Technol.*, 2018, **267**, 1–8.
139 X. Wang, X. Liu, C. Xiao, H. Zhao, M. Zhang, N. Zheng, W. Kong, L. Zhang, H. Yuan, L. Zhang and J. Lu, *Microporous Mesoporous Mater.*, 2020, **297**, 110041.
140 C. Zheng, H. Zheng, Y. Sun, B. Xu, Y. Wang, X. Zheng and Y. Wang, *Bioresour. Technol.*, 2019, **293**, 122038.
141 J. d. O. Marques Neto, C. R. Bellato and D. d. C. Silva, *Chemosphere*, 2019, **218**, 391–401.
142 Y. Mu, Z. Ai, L. Zhang and F. Song, *ACS Appl. Mater. Interfaces*, 2015, **7**, 1997–2005.
143 S. Shi, J. Yang, S. Liang, M. Li, Q. Gan, K. Xiao and J. Hu, *Sci. Total Environ.*, 2018, **628–629**, 499–508.
144 S. Ji, C. Miao, H. Liu, L. Feng, X. Yang and H. Guo, *Nanoscale Res. Lett.*, 2018, **13**, 178.
145 L. V. Alves Gurgel, J. C. Perin de Melo, J. C. de Lena and L. F. Gil, *Bioresour. Technol.*, 2009, **100**, 3214–3220.
146 F. Karimi, A. Ayati, B. Tanhaei, A. L. Sanati, S. Afshar, A. Kardan, Z. Dabirifar and C. Karaman, *Environ. Res.*, 2022, **203**, 111753.
147 M. F. Mubarak, A. H. Ragab, R. Hosny, I. A. Ahmed, H. A. Ahmed, S. M. El-Bahy and A. El Shahawy, *Polymers*, 2021, **13**, 2714.
148 F. Rahmi, F. P. Lelifajri and R. Sembiring, *IOP Conf. Ser.: Mater. Sci. Eng.*, 2019, **276**, 012004–012007.
149 M. Omidinasab, N. Rahbar, M. Ahmadi, B. Kakavandi, F. Ghanbari, G. Z. Kyzas, S. Silva Martinez and N. Jaafarzadeh, *Environ. Sci. Pollut. Res.*, 2018, **25**, 34262–34276.
150 H. Li, F.-X. Zhou, B.-H. He, G.-X. Wang, W.-Y. Xie and E. Liang, *ChemistrySelect*, 2020, **5**, 8033–8039.
151 D. Yuan, W. Zhang, J. Cui, L. He, J. Wang, C. Yan, Y. Kou and J. Li, *Environ. Sci. Pollut. Res.*, 2020, **27**, 2588–2598.
152 F. Qi, Z. Dong, D. Lamb, R. Naidu, N. S. Bolan, Y. S. Ok, C. Liu, N. Khan, M. A. H. Johir and K. T. Semple, *Chemosphere*, 2017, **180**, 564–573.
153 K. Hachem, S. A. Jasim, M. E. Al-Gazally, Y. Riadi, G. Yasin, A. T. Jalil, M. M. Abdulkadhm, M. M. Saleh, M. N. Fenjan, Y. F. Mustafa and A. D. Khalaji, *J. Chin. Chem. Soc.*, 2022, **69**, 512–521.
154 H. H. Najafabadi, M. Irani, L. R. Rad, A. H. Haratameh and I. Haririan, *RSC Adv.*, 2015, **5**, 16532–16539.
155 L. Zhou, Y. Liu, S. Liu, Y. Yin, G. Zeng, X. Tan, X. Hu, X. Hu, L. Jiang, Y. Ding, S. Liu and X. Huang, *Bioresour. Technol.*, 2016, **218**, 351–359.
156 M. Zhang, Z. Zhang, Y. Peng, L. Feng, X. Li, C. Zhao and K. Sarfaraz, *Int. J. Biol. Macromol.*, 2020, **156**, 289–301.
157 P. Sun, W. Zhang, B. Zou, L. Zhou, Z. Ye and Q. Zhao, *Int. J. Biol. Macromol.*, 2021, **182**, 1138–1149.
158 W. Cai, F. Zhu, H. Liang, Y. Jiang, W. Tu, Z. Cai, J. Wu and J. Zhou, *Chem. Eng. Res. Des.*, 2019, **144**, 150–158.
159 X. Song, L. Li, L. Zhou and P. Chen, *Chem. Eng. Res. Des.*, 2018, **136**, 581–592.